Mon. Not. R. astr. Soc. (1990) **242,** 167–176 and *Microfiche* MN 242/1

The giant branch of the Fornax dwarf spheroidal galaxy

Ram Sagar[1], M. R. S. Hawkins[2] and R. D. Cannon[3]

[1] *Indian Institute of Astrophysics, Bangalore 560034, India*
[2] *Royal Observatory, Blackford Hill, Edinburgh EH9 3HJ, Scotland*
[3] *Anglo-Australian Observatory, PO Box 296, Epping, NSW 2121, Australia*

Accepted 1989 June 12. Received 1989 May 15; in original form 1989 January 30

SUMMARY

A colour–magnitude diagram for a large sample of stars in the Fornax dwarf spheroidal galaxy has been obtained from BV electronographic observations. These reach to the level of the horizontal branch, below $V=21$ mag. The area of investigation is located ~18 arcmin away in a south-west direction from the centre of the Fornax galaxy. The wide field of the McMullan camera enabled some 1300 stars to be measured and made possible an analysis of structure in the giant branch. The standard deviation of the intrinsic width of the giant branch is ~0.14 mag in $(B-V)$ colour at a given luminosity, which yields a standard deviation of 0.3 in [Fe/H], if a spread in metallicity alone is responsible for the intrinsic width. Otherwise a combination of both variation in age from 3 to 17 billion yr and a spread in metallicity equivalent to a standard deviation of 0.27 in [Fe/H] can account for the intrinsic width of the giant branch. A comparison with galactic globular clusters as well as theoretical isochrones suggests a mean value of [Fe/H] $= -1.5 \pm 0.1$ for the Fornax giant branch stars.

1 INTRODUCTION

Seven ghostly collections of stars known as dwarf spheroidal galaxies are found in the outer halo of the Milky Way, and provide useful laboratories for the study of the galaxian stellar content and star formation history, and for the testing of current stellar evolutionary ideas. The Fornax dwarf spheroidal (A0237−34) was first recognized on Harvard plates by Shapley (1938). It has a number of distinguishing characteristics among the population of galactic dwarf spheroidals, being the most luminous in integrated light ($M_V \sim -12$ mag), the largest in diameter (~3 kpc) and the brightest in central surface intensity. It is also the least massive galaxy known to possess globular clusters (Harris & Racine 1979; Harris & van den Bergh 1981). Its mass lies midway between that of galactic globular clusters and nearby dwarf irregular galaxies.

Many investigators (Demers & Kunkel 1979; Westerlund 1979; Aaronson & Mould 1980; Frogel *et al.* 1982; Richer & Westerlund 1983; Azzopardi & Westerlund 1984; Westerlund, Edvardsson & Lundgren 1987, and references therein) have found carbon stars and other types of red stars in the field of the Fornax dwarf galaxy, which show a wide range in observed $(B-V)$ colour at a given luminosity. Colour magnitude diagrams (CMDs) of the field stars in Fornax have been presented by Demers, Kunkel & Hardy (1979) and later by Buonanno *et al.* (1985b) using the same photographic material and photoelectric sequence. However, the latter used more sophisticated techniques for measuring stellar images and hence have been able to do reasonably precise photometry for stars ~2 mag fainter than the former, and also to measure more crowded stars. Deep (to $V=24.3$ mag) V, $(B-V)$ CMDs based on CCD observations have been presented by Gratton, Ortolani & Richter (1986a) and by Light & Seitzer (1988). These CMDs show a wide giant branch comparable to that of the anomalous galactic globular cluster ω Cen (NGC 5139; Cannon & Stobie 1973) and probably indicate a significant spread in metallicity as well as perhaps in age. A range in metallicity and age in the globular clusters of the Fornax dwarf has also been suggested by many workers either on the basis of integrated light observations (van den Bergh 1969; Danziger 1973; Zinn & Persson 1981; Jones & Hyland 1982; Gordon & Kron 1983, and references therein) or based on the location of the giant branch in the CMD (Verner *et al.* 1981; Buonanno *et al.* 1985b). The CMDs of the Fornax dwarf globular clusters given by Verner *et al.* (1981) are based on photographic photometry while those by Buonanno *et al.* (1985b) are based on both photography and CCD photometry. These studies indicate that most of the field star population in Fornax is more metal-rich than the globular clusters themselves.

For population II objects, the structure of the giant branch down to and including the horizontal branch provides a useful measure of distance and metallicity. In spite of considerable observational efforts made during the last few

years, no large-scale photometric study of the giant branch of the field stars of the Fornax dwarf has been made. The present work gives electronographic observations down to $V=21$ mag in both B and V photometric bands, for a sufficiently large number (~ 1300) of stars to achieve this. Although electronography has to some extent been superseded recently by CCD photometry, it remains practically useful for applications such as the present one where it is necessary to cover large fields in order to get big enough samples of stars, and has the great advantage over photography that it has a linear response and hence yields calibrated data. Although the present data are of lower accuracy than the best CCD data, they are adequate to quantify the wide spread on the giant branch found earlier by Demers *et al.* (1979), Buonanno *et al.* (1985b) and Light & Seitzer (1988), and they show that the horizontal branch is located at $V\sim$ 21.4 mag near the limit of our observations, as has been confirmed recently for smaller samples of stars by Buonanno *et al.* (1985b) and Gratton *et al.* (1986a).

2 OBSERVATIONS AND REDUCTIONS

The electronographic observations were carried out on the 1.5-m Danish telescope, La Silla, Chile using the 8-cm McMullan electronographic camera and Ilford L4 emulsion, which gives a plate scale of 16.2 arcsec mm^{-1}. All films were exposed for 60 min. The main programme stars were measured on a set of 2 V and 2 B exposures obtained in 1979 November, and additional offset exposures were obtained in 1981 and 1982 to connect to a larger number of photoelectric standards.

The area investigated is $\sim 11\times 11$ arcmin square centred near star 11365 of Demers *et al.* (1979), which is ~ 18 arcmin south-west from the centre of Fornax and includes cluster 2 (Plate 1). In addition, a number of flat-field exposures of the twilight sky were obtained during each observing run. The exposures taken with offset centres were used to tie the programme star exposures in with the photoelectric observations of Demers *et al.* (1979). The electronographic films were scanned on the RGO PDS microdensitometer using the techniques described by Penny (1984). The high precision and measuring speed of this machine, and automatic nature of its operation, make it a useful tool for photometric studies of large numbers of stars. A scan speed of 23.5 mm s^{-1} and a 24-μm square measuring aperture with 20-μm steps in both x and y directions was used for the flat field exposures. The programme and calibration exposures were scanned at a slower speed of 5 mm s^{-1} with an 11-μm square measuring aperture using 10-μm steps. Some image distortion is generally found near the edge of the field of the 8-cm McMullan electronographic camera, and so the observations were confined to within about 25 mm of the field centre, which was well clear of any such effect. For the programme exposures, four areas each of 2048×2048 pixel, and for the calibration exposures three smaller areas of 512×512, 700×800 and 50×1200 pixel were scanned. In order to measure the clear film level and to check for the PDS zero-point drift during the scan, measurements were made in the 'multi-segmented' mode of the PDS. In this mode, the scan was automatically interrupted approximately every ten minutes during a five-hour measuring run in order to perform a 30×30 raster scan on a fixed reference area of the film which had been exposed to the cathode background flux, but not to the sky. The STARLINK programs written by Penny were used to reduce the data. All the reductions were done on the VAX 11/780 of the Royal Observatory, Edinburgh. The photocathode non-uniformity corrections obtained from the flat fields turned out to be quite small, about 5 per cent over the measured area for both B and V. These corrections were applied to the programme and calibration exposures in the same way as described by Sagar, Cannon & Hawkins (1988) for the globular cluster NGC 1851.

The star magnitudes were determined by a profile-fitting procedure. Small areas around each star were fitted with a Gaussian profile using a two-dimensional iterative linearized least-squares fitting procedure. The density measures so obtained are linearly related to flux, and this relation has been extensively checked in earlier work for the system in use here (e.g. Hawkins 1981). By comparing the electronographic magnitudes of 17 stars with photoelectric values in the range of $V=13.0$–18.5 mag and $(B-V)=0.4$–1.8 mag, the linearity of the present electronographic system has also been confirmed by Sagar *et al.* (1988). The colour equations for the camera given earlier by us (Sagar *et al.* 1988) for the globular cluster NGC 1851 have been used in this work, as both objects were observed during the same observing runs. The zero-point of the photometric system for Fornax has been determined using stars L, M, S, T, 6673, 6771, 7353, 11232, 11239, 11325 and 11505 of Demers *et al.* (1979). As most of the stars used for zero-point estimation are faint ($B\geq 19$ mag) and have been observed photoelectrically only once by Demers *et al.* (1979), the errors on the zero-point are ± 0.06 mag.

Table 1 (on microfiche MN 242/1) gives the relative positions of the stars measured in arcsecs, together with the electronographic V and $(B-V)$ magnitudes, of all the stars measured in four areas (marked R1–R4 in Plate 1) of the Fornax dwarf galaxy. The stars observed by other investigators are also identified in Table 1. The relative positions are measured with respect to star R1 − 107 (= DK 7 = star 11365 of Demers *et al.* 1979) and have an internal accuracy of 1 arcsec. The scale and orientation of the coordinate system were initially established with respect to some of the stars for which positions are given by Westerlund, Edvardsson & Lundgren (1987), and later confirmed by astrometric measurements relative to a set of Perth 70 and SAO stars on a film copy of the SERC(J) plate of field 356 in the ESO/SERC Southern Sky Survey. The measured position of star R1 − 107 for 1950 is $\alpha=02^{h}36^{m}52^{s}.8$, $\delta=-35^{\circ}00'42''$ and independent checks on a small sample of the programme stars indicate that the positions given have an external accuracy within 2 arcsec. Table 1 lists the BV magnitudes of only those stars which were measured on all four exposures. A few measured stars have been identified in Plate 1.

The internal standard deviations (σ) for the present photometry based on film-to-film scatter, in magnitude bins, are shown in Table 2. It will be seen that the errors are less than 0.03 mag for $V<19$ mag and $B<20.6$ mag, but that they increase with magnitude thereafter, becoming 0.13 mag for $V\sim 21$ mag and $B\sim 22$ mag. For stars fainter than this, σ is very large and the observations must be considered unreliable.

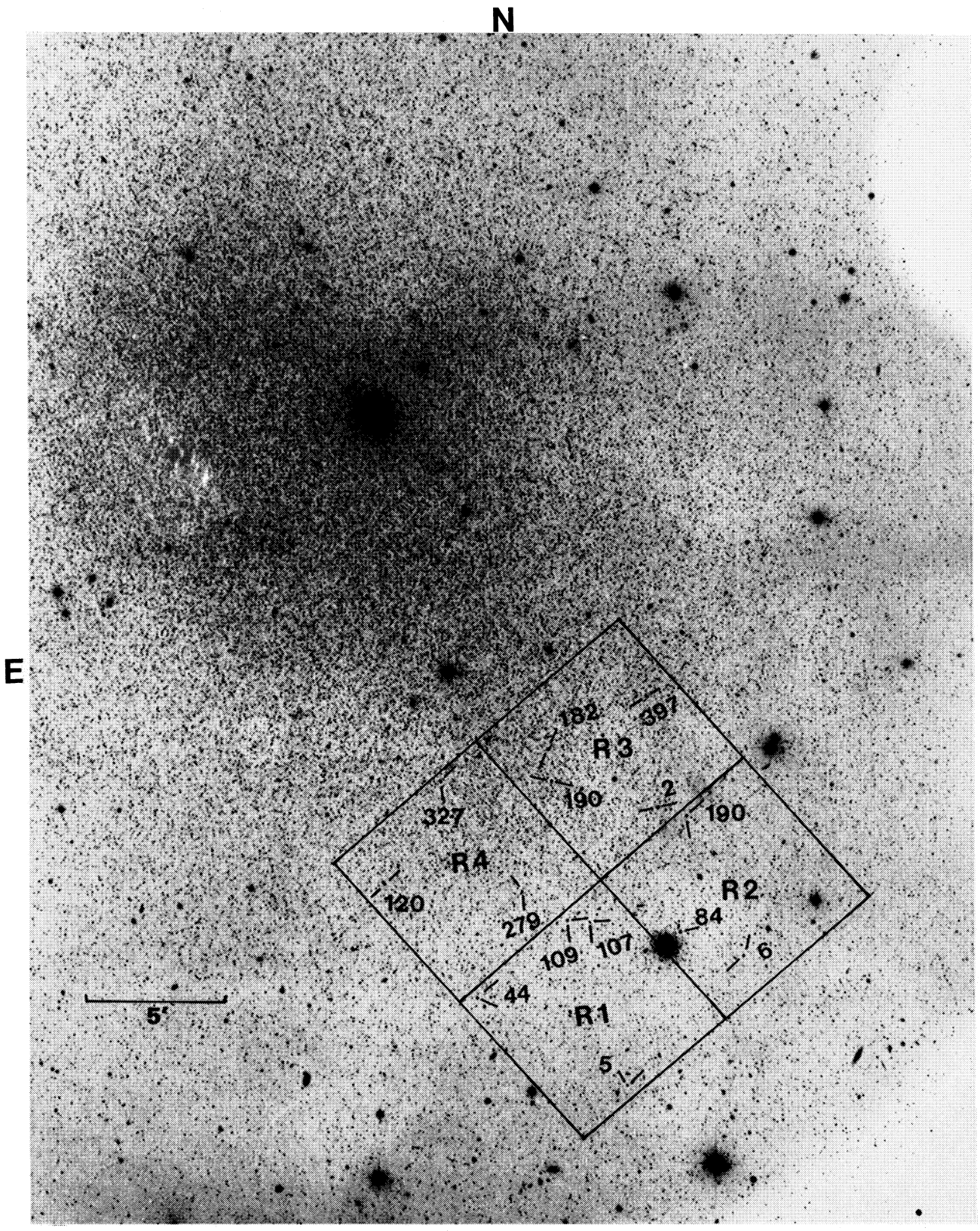

Plate 1. Regions R1–R4 were scanned on the electronographic films. In each region a few measured stars have been identified. Two bright stars SAO 193841 and 193835 are located respectively near the centre of the Fornax dwarf and the south-west corner of the plate. This photograph has been reproduced from a IIIa-J AAT plate which was exposed for 80 min through a GG 385 filter and sub-beam prism. The latter has produced ~ 7 mag fainter ghost images of bright stars.

[*facing page* 168]

Table 2. Internal precision of the photometry.

V range	σ_V	B range	σ_B
< 18.5	0.02	< 20.0	0.03
18.5 - 19.0	0.03	20.0 - 20.6	0.03
19.0 - 19.5	0.05	20.6 - 20.8	0.04
19.5 - 20.0	0.07	20.8 - 21.0	0.05
20.0 - 20.5	0.10	21.0 - 21.4	0.07
20.5 - 21.0	0.13	21.4 - 22.0	0.10
21.0 - 21.4	0.14	22.0 - 22.2	0.13
21.4 - 21.8	0.18	22.2 - 22.4	0.16
> 21.8	0.28	> 22.4	0.22

The external accuracy is difficult to estimate because it depends on the accuracy of the photoelectric sequence. However, it seems unlikely that the sequence will be systematically in error by more than a few hundredths of a magnitude.

2.1 Comparison with other photometry

The stars common in between the present observations and those of Verner *et al.* (1981) and Buonanno *et al.* (1985b) make possible a comparison of the photometry. In Fig. 1, we plot the differences in the sense 'present' minus 'others' against brightness in both B and V. The present data agree very well (see also Table 3) with those given by Buonanno *et al.* They also appear to be in fair agreement with the Verner *et al.* observations for stars brighter than $V=20$ mag and $B=21$ mag, but systematically increasing differences with magnitude in both B and V exist for fainter stars, reaching $\Delta V\sim 1$ mag at $V=21.7$ mag and $\Delta B\sim 0.6$ mag at $B=22.3$ mag. In order to check whether these differences are real or due to the few stars in common between the present and Verner *et al.* photometries, the two previously published sets of data, which have many stars in common, have been compared in Fig. 2. Although both use the same photographic material and photoelectric sequence, the BV magnitudes listed by Buonanno *et al.* are assumed to be more accurate and reliable because they have used a more refined technique in measuring the stellar images and have also carried out CCD observations for some stars. The two sets of observations agree very well for stars brighter than $V=20.2$ mag and $B=21.4$ mag, but differ systematically in the same way as in Fig. 2 for fainter stars in both B and V. The differences in the sense Buonanno *et al.* minus Verner *et al.*

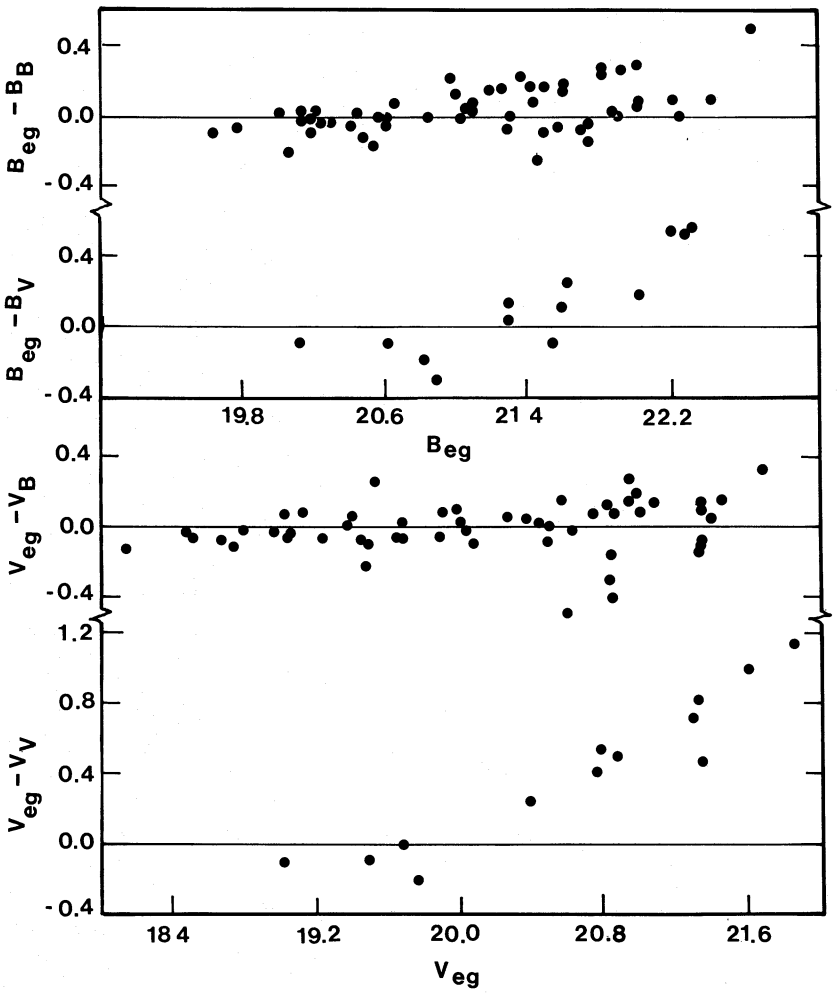

Figure 1. Comparison of present data with those of Buonanno *et al.* (1985b) and Verner *et al.* (1981). The subscripts 'eg', 'B' and 'V' mean the present electronographic data, the data by Buonanno *et al.* and by Verner *et al.*, respectively.

Table 3. The mean and standard deviation of the photometric differences in the sense 'present' minus 'Buonanno *et al.*' (1985b).

V range (mag)	Mean ± S.d. (mag) (mag)	n	B range (mag)	Mean ± S.d. (mag) (mag)	n
18.0 - 19.0	-0.07 ± 0.04	7	19.6 - 20.2	-0.07 ± 0.07	8
19.0 - 19.4	-0.01 ± 0.07	6	20.2 - 20.6	-0.05 ± 0.07	9
19.4 - 19.8	-0.01 ± 0.13	9	20.6 - 21.0	0.05 ± 0.10	6
19.8 - 20.2	0.00 ± 0.08	6	21.0 - 21.4	0.06 ± 0.10	9
20.2 - 20.6	0.03 ± 0.07	6	21.4 - 21.6	0.03 ± 0.16	8
20.6 - 21.0	-0.06 ± 0.23	12	21.6 - 22.0	0.08 ± 0.18	9
21.0 - 21.6	0.03 ± 0.12	9	22.0 - 22.4	0.06 ± 0.14	6

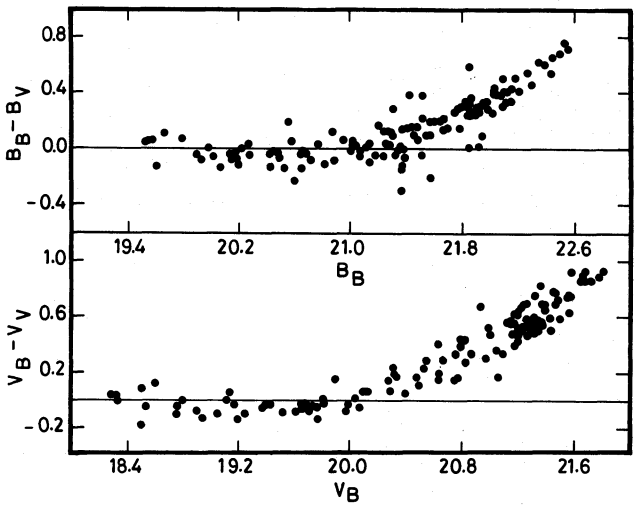

Figure 2. Comparison of the data by Buonanno *et al.* (1985b) with those by Verner *et al.* (1981). The subscripts mean the same as in Fig. 1.

become $\Delta V \sim 0.9$ mag at $V = 21.7$ mag and $\Delta B \sim 0.7$ mag at $V = 22.5$ mag, very similar to the results found above. It appears most likely that the two independent recent sets of data are correct, and that the errors lie mainly in the earlier photographic work of Verner *et al.* (1981).

3 COLOUR–MAGNITUDE DIAGRAM

Fig. 3 shows the V, $(B-V)$ colour–magnitude diagram (CMD) of the present observations. The great concentration of stars at $V \sim 21.4$ mag looks like the horizontal branch although it is unfortunate that our measuring errors are becoming large at this level and the feature lies immediately above our magnitude limit. Its identification is confirmed by the recent deep and relatively precise photometry of the Fornax globular clusters and field stars by Buonanno *et al.* (1985b) and Gratton *et al.* (1986a). The apparent redward extension of the horizontal branch is probably due to the large measuring errors and the very large number of stars with $V > 21$ mag, and it is not possible to define its mean position unambiguously.

Before discussing the other features of the CMD it is worthwhile establishing the contamination by foreground stars in our Galaxy. The number of galaxian stars in the direction of the Fornax dwarf galaxy has been estimated using Ratnatunga & Bahcall's (1985) predictions and their distribution in the CMD is listed in Table 4. We expect 10 such stars in our sample of stars brighter than $V = 17$ mag and another 44 among the fainter stars up to $V = 21$ mag. This constitutes a contamination of only 8 per cent in the whole CMD and much less than that along the giant branch; such contamination is much too small to affect the conclusions of the present work.

Demers & Kunkel (1979) and Westerlund *et al.* (1987) have identified 245 very red stars in the Fornax dwarf galaxy.

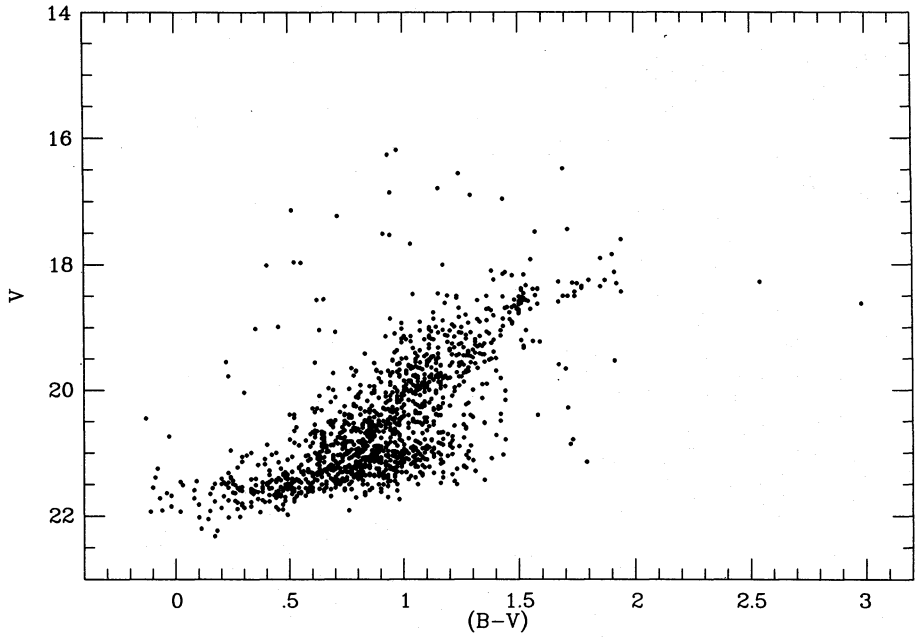

Figure 3. The $V, (B-V)$ electronographic colour–magnitude diagram of the stars of the Fornax dwarf spheroidal galaxy.

Table 4. Predicted and observed distribution of field stars in the colour-magnitude diagram.

	Total		(B-V) < 0.82 mag		0.82 mag ≤(B-V) ≤ 1.32 mag		(B-V) > 1.32 mag	
Range in V mag	Expected field stars	Observed in CMD	Expected field stars	Observed in CMD	Expected field stars	Observed in CMD	Expected field stars	Observed in CMD
13-15	3	0	2	0	1	0	0	0
15-17	7	8	3	0	3	6	1	2
17-19	14	113	5	8	3	28	6	77
19-21	30	663	11	149	4	470	15	44
21-23	50	503	10	335	11	164	29	4

Table 5. Known very red stars observed electronographically.

	Present		Demers & Kunkel (1979)			Westerlund *et al.* (1987)			
Star	V (mag)	(B-V) (mag)	Star	V (mag)	(B-V) (mag)	Star	V (mag)	(B-V) (mag)	Spectral type
R1,107	18.27	2.54	7	18.08	2.48	DK 7	18.30	2.30	Carbon star[2]
R1,132	18.62	2.98	8	19.08	2.38	DK 8	19.2	2.2	
R2,82	18.49	1.57	9	18.41	1.75	DK 9	18.37	1.69	
R3,25	18.25	1.87	13	18.14	1.64	DK 13	18.11	1.84	
R3,397	16.48	1.69				BM 25	16.20	1.95	M[1]
R4,62	17.60	1.94	6	17.47	2.02	DK 6	17.50	1.78	Continuum[2]
R4,155	17.90	1.85	24	17.91	2.11	DK 24	18.00	2.09	M[1]
R4,182	18.12	1.91	11	18.31	1.82	DK 11	18.29	1.87	
R4,183	18.34	1.77	12	18.42	1.68	DK 12	18.37	1.77	
R4,327	16.96	1.43				WEL 25	16.61	1.89	M[1]

[1]From Westerlund *et al.* (1987). [2]From Aaronson & Mould (1980).

Table 6. Mean points for the giant branch of Fornax.

<V> (mag)	<B-V> (mag)	n	Dispersion in (B-V) σ_O (mag)	σ_E (mag)	σ_I (mag)
18.30±0.02	1.66±0.04	17	0.157	0.036	0.15±0.03
18.54±0.01	1.49±0.03	29	0.151	0.042	0.15±0.02
18.77±0.01	1.38±0.02	27	0.122	0.042	0.12±0.02
19.05±0.01	1.21±0.03	37	0.156	0.058	0.15±0.02
19.28±0.01	1.19±0.02	39	0.126	0.058	0.11±0.02
19.53±0.01	1.16±0.02	62	0.124	0.064	0.11±0.01
19.78±0.01	1.08±0.02	66	0.140	0.081	0.11±0.02
20.02±0.01	1.01±0.02	72	0.144	0.099	0.11±0.02
20.29±0.01	0.97±0.02	79	0.164	0.122	0.11±0.02
20.53±0.01	0.90±0.02	103	0.162	0.141	0.08:
20.79±0.01	0.87±0.02	119	0.196	0.164	0.11:

Ten of these stars have been observed in the current work. Their photometry by various investigators and their spectral classifications are listed in Table 5. Only one is a known carbon star, another one is a featureless star, another three are M-type stars and for the remaining stars, including the reddest in our sample, the spectral types are unknown. A comparison of the various V and $(B-V)$ values indicates that in most cases agreement is satisfactory. In a few cases, the discrepancies are large which could be because of the variability of stars, although it is notoriously difficult to avoid systematic colour errors when measuring such cool stars.

The remainder of this section is devoted to an estimate of the true width of the giant branch (GB) and to relating its structure to the metallicity and age parameters of the Fornax dwarf galaxy.

3.1 The intrinsic width of the giant branch

It is clear from Fig. 3 that the GB is exceptionally broad. Due to the large sample of stars, the width can be better determined than in the CMDs of Demers *et al.* (1979), Buonanno *et al.* (1985b) and Gratton *et al.* (1986a). The appearance of the giant branch in the CMD is the same even if only stars having film-to-film scatter ≤0.10 mag (i.e. relatively precise measurements) are considered, which suggests that the width is indeed intrinsic. Light & Seitzer (1988) have also drawn a similar conclusion on the basis of BVR CCD photometry. They also found that the intrinsic dispersion remains roughly constant with respect to radial distance from the centre of Fornax. To quantify the intrinsic dispersion, a simple analysis has been carried out. The stars have been binned in 0.25 mag intervals in V and the average $(B-V)$ and dispersion σ_O have been estimated for each bin. A few stars lying more than 2.5 σ_O away from the mean of each bin were not included in the calculation. These results are given in Table 6. Because of the large errors and the presence of the horizontal branch at $V\sim$ 21.4 mag, the analysis has not been carried out for stars fainter than $V=21$ mag. The expected scatter in $(B-V)$ at any given V, σ_E, arising purely from the internal uncertainty of the photometry, is also listed in Table 6. Assuming Gaussian distributions for σ_O and σ_E, the intrinsic width of the giant branch in $(B-V)$, σ_I, is estimated as $\sigma_I^2=\sigma_O^2-\sigma_E^2$. The variation of σ_O and σ_E with V is shown in Fig. 4. As a statistically significant difference exists between σ_O and σ_E for $V<20.3$ mag, the estimates of σ_I should be considered reliable down to this limit. In the range $V=18.3$–20.3 mag, the values of σ_I are nearly the same within the errors. The present analysis implies a significant intrinsic width in the $(B-V)$ colours of

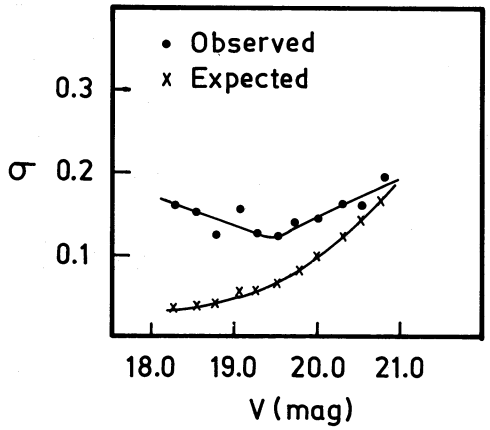

Figure 4. The observed dispersion σ_O and the dispersion σ_E expected from the internal errors of the photometry are plotted against V along the giant branch, as listed in Table 6.

the giants at a given luminosity level since the field star contamination is very little along the giant branch (*cf.* Table 4). This simple analysis ignores the probable contribution of asymptotic giant branch (AGB) stars to the scatter in the CMD. Comparison with galactic star clusters indicates that such a contribution should be small at least down to $V=20$ mag.

3.1.1 *Comparison with other dwarf spheroidal galaxies*

Fig. 5 gives a comparison of the mean locus of the Fornax giant branch with those of other dwarf spheroidal galaxies, shifting them to have the same distance and reddening as Fornax. An apparent distance modulus of 20.7 mag and a reddening of $E(B-V)=0.03$ have been adopted for the Fornax dwarf (*cf.* Buonanno *et al.* 1985b; Gratton *et al.* 1986a). The giant branch, apparent distance modulus and reddening data for Carina, Draco, Leo I, Leo II , Sculptor and Ursa Minor have been taken from Godwin (1986), Stetson (1979), Fox & Pritchet (1987), Demers & Harris (1983), Kunkel & Demers (1977) and Schommer, Olszewski & Cudworth (1981), respectively. In comparison to the Fornax giant branch, all other dwarf spheroids have bluer and steeper giant branches except Leo I and Leo II.

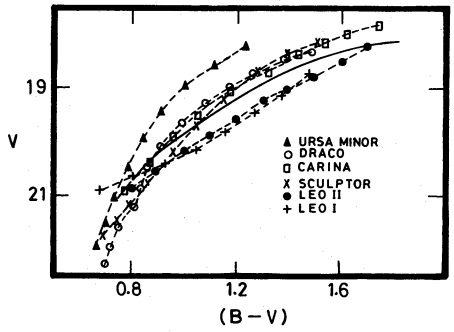

Figure 5. The ridge line of the Fornax dwarf (continuous curve) compared with those of other dwarf spheroidals.

3.1.2 *Comparison with galactic globular clusters*

Fig. 6 shows the giant branches of three galactic globular clusters, namely M92, M3 and 47 Tuc (NGC 104) having $[Fe/H]=-2.24\pm0.08$, -1.66 ± 0.06 and -0.71 ± 0.08, respectively on the scale of Zinn & West (1984), superimposed on the Fornax giant branch. The giant branch, distance modulus and reddening data for M3 and M92 are taken from Sandage (1970) while those for NGC 104 are from Hesser *et al.* (1987). This figure shows that the mean Fornax giant branch is very similar in slope to those of galactic globular clusters, and the range in metallicity of the Fornax giant stars is as large as that between the galactic globular clusters (i.e. $-2.2\leq[Fe/H]\leq-0.7$), if one attributes a spread of $\pm2\ \sigma_1$ in the giant branch to differences in metallicity.

3.1.3 *Comparison with theoretical giant branch loci*

The shape of the Fornax GB can be compared with the revised theoretical Yale isochrones published recently by

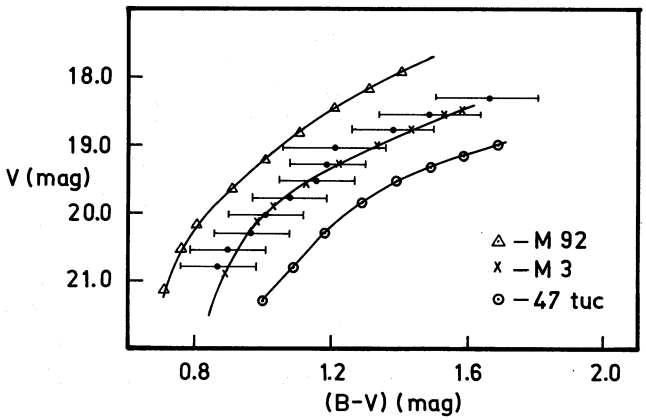

Figure 6. The ridge line of Fornax superimposd on the ridge lines of the giant and horizontal branches of the galactic globular clusters M92, M3 and 47 Tuc. The bars indicate one sigma intrinsic dispersions in $(B-V)$.

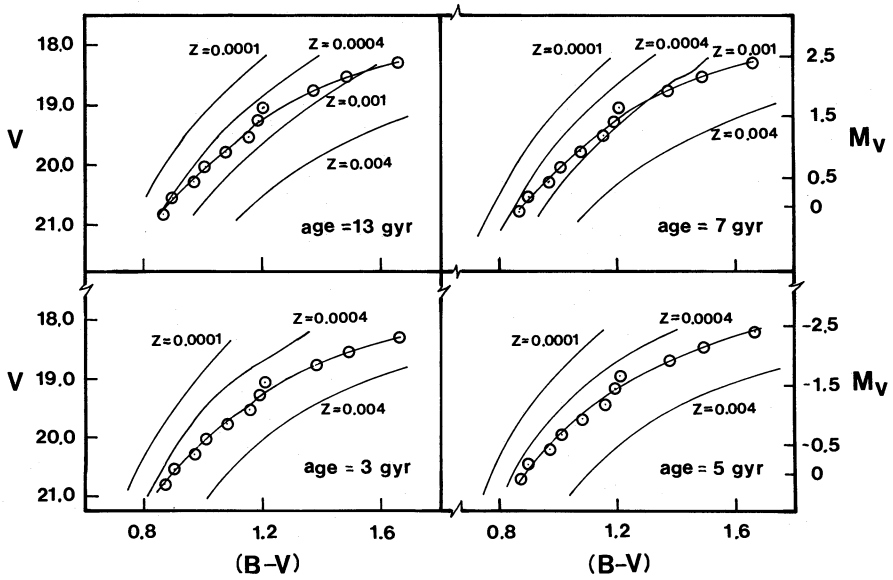

Figure 7. Comparison of theoretical isochrones given by Green *et al.* (1987) with the giant branch of Fornax.

Green, Demarque & King (1987). The isochrones for [Fe/H] = −0.7 (z = 0.004), −1.3 (z = 0.001), −1.7 (z = 0.0004), −2.3 (z = 0.0001), and age = 3, 5, 7, 13 Gyrs, have been superimposed on the Fornax GB in Fig. 7. A helium abundance of Y = 0.2 has been used in this comparison; the use of Y = 0.3 does not change the conclusions. It is apparent that differences in metallicity are much more significant than differences in age, and that age variations alone cannot explain the width of the Fornax GB (see also Aaronson & Mould 1980, 1985). The mean location of the Fornax GB is perhaps best fitted by the 5 Gyr theoretical isochrones, where it lies between the isochrones for [Fe/H] = −1.7 and [Fe/H] = −0.7. It is interesting to note that an age of 2–4 Gyr has been assigned to the Fornax field stars by Gratton *et al.* (1986a) on the basis of the location of the main-sequence turn-off point in the V, $(B-V)$ diagram. This is of course much younger than the age of galactic globular clusters, but as noted above it appears that changes in age produce only small changes in the location of the GB.

3.2 The metallicity

The mean metallicity and the spread in metallicity of field stars in the Fornax dwarf have been estimated respectively from the mean position and intrinsic width of its red giant branch (RGB), using an empirical calibration of [Fe/H] versus $(B-V)$ for the GB as well as the Yale theoretical isochrones. The results are described below.

The analysis has been done using stars in the interval 18.8 mag ≤ V ≤ 19.8 mag. In this interval statistically significant numbers of stars (201) are present and the photometry is relatively reliable. This interval also avoids the considerable confusion between RGB, horizontal branch and possible asymptotic branch (AGB) stars that occurs for V > 20.5 mag (Buonanno *et al.* 1985b; Gratton *et al.* 1986a). The method outlined in Section 3.1 has been used to estimate the mean position and intrinsic width of the RGB. The mean position of the RGB is $\langle B-V\rangle = 1.16 \pm 0.02$ mag [using $E(B-V) = 0.03$ mag]. The distribution of residuals in 0.05 mag bins in $(B-V)$ is shown in Fig. 8, which is adequately matched by a Gaussian distribution with $\sigma = 0.15$ mag. The expected scatter in $(B-V)$ due to measuring errors is 0.06 mag in the range V = 18.8–19.8 mag. Hence, the intrinsic dispersion in $(B-V)$ is 0.14 ± 0.01 mag. A relationship between [Fe/H] and the RGB intrinsic colour at $M_V = -1.4$ mag (the middle point of the V interval) is then used to transform $\langle B-V\rangle$ and σ_I into mean and standard deviation in [Fe/H], respectively. The relationship is derived from the CMDs of 15 galactic globular clusters listed in Table 7. Metallicities for NGC 3201, 4590, 5272, 6171, 6205, 6341, 7078 and 7099 are taken from Zinn & West (1984). For others, those given by Gratton *et al.* (1986b), Gratton (1987) and Wallerstein & Leep (1987) are used as they are based on high-resolution spectra. They agree within ±0.1 dex with the ones given by Zinn & West (1984) except for NGC 6838 where the difference is 0.23 dex. Precise locations of the

Table 7. [Fe/H] and $(B-V)_0$ of the giant branch at $M_v = -1.4$ mag of a sample of galactic globular clusters, along with the reddening $E(B-V)$, apparent distance modulus $(m-M)_v$ and the sources of data.

Cluster	[Fe/H]	Source for col. 2	$(B-V)_0$ (mag)	E(B-V) (mag)	$(m-M)_v$ (mag)	Sources for cols. 4,5,6
NGC 104 (47 Tuc)	-0.82	1	1.48	0.04	13.4	2
NGC 288	-1.31	3	1.24	0.03	14.6	4,24
NGC 362	-1.18	3	1.22	0.04	14.8	5,6
NGC 3201	-1.61	7	1.15	0.22	14.1	8
NGC 4590 (M 68)	-2.09	7	0.86	0.07	15.3	9
NGC 5272 (M 3)	-1.66	7	1.21	0.01	14.8	10
NGC 5904 (M 5)	-1.42	1	1.19	0.03	14.5	11
NGC 6121 (M 4)	-1.20	12	1.40	0.37	12.5	13,14
NGC 6171 (M 107)	-0.99	7	1.35	0.38	14.8	15,16
NGC 6205 (M 13)	-1.60	12	1.08	0.02	14.5	17,18
NGC 6341 (M 92)	-2.24	7	0.99	0.02	14.4	19
NGC 6752	-1.53	1	1.08	0.04	13.3	20
NGC 6838 (M 71)	-0.81	1	1.50	0.27	13.7	21
NGC 7078 (M 15)	-2.15	7	0.84	0.11	15.5	22
NGC 7099 (M 30)	-2.13	7	0.94	0.04	14.7	23

Reference numbers. 1 = Gratton *et al.* (1986b); 2 = Hesser *et al.* (1987); 3 = Gratton (1987); 4 = Buonanno *et al.* (1984); 5 = Harris (1982); 6 = Bolte (1987a); 7 = Zinn & West (1984); 8 = Alcaino & Liller (1981); 9 = McClure *et al.* (1987); 10 = Buonanno *et al.* (1986); 11 = Buonanno *et al.* (1981); 12 = Wallerstein & Leep (1987); 13 = Lee (1977); 14 = Richer & Fahlman (1984); 15 = Dickens & Rolland (1972); 16 = Da Costa *et al.* (1984); 17 = Sandage (1970); 18 = Richer & Fahlman (1986); 19 = Buonanno *et al.* (1985a); 20 = Penny & Dickens (1986); 21 = Cudworth (1985); 22 = Fahlman, Richer & VandenBerg (1985); 23 = Bolte (1987b); 24 = Pound, Janes & Hearley (1987).

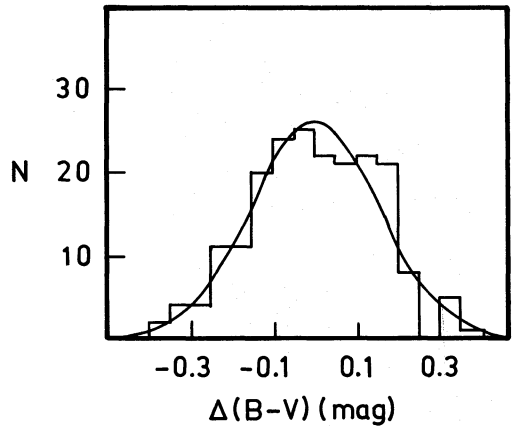

Figure 8. Histogram of the distribution of residuals in $(B-V)$ from the Fornax mean giant branch in the region 18.8 ≤ V ≤ 19.8 mag. The smooth curve is a Gaussian distribution with standard deviation of 0.151 mag.

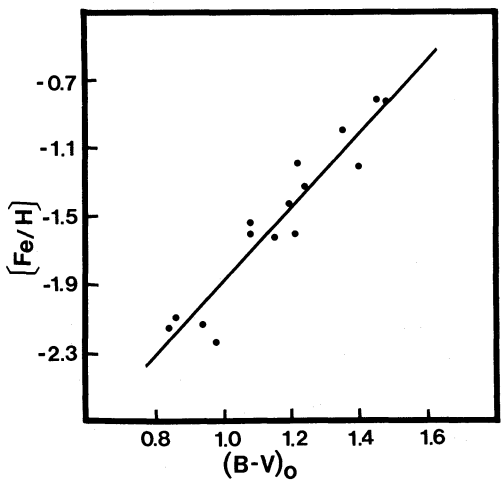

Fig. 9. Plot of [Fe/H] versus $(B-V)_0$ of the red giant branch at $M_V = -1.4$ mag, for a sample of galactic globular clusters.

RGB, reddening and distance estimates (mainly from modern CCD photometry) are taken from the sources listed in Table 7. An [Fe/H] versus $(B-V)_0$ plot is shown in Fig. 9. The empirical relation derived using least-squares linear regression is

$$[\mathrm{Fe/H}] = -4.05(\pm 0.38) + 2.16(\pm 0.21)(B-V)_0. \quad (1)$$

This procedure yields a mean metallicity [Fe/H] $= -1.5$ (± 0.37) and a standard deviation in [Fe/H] of 0.30 (± 0.14) in Fornax, if one assumes that the intrinsic width of the GB is only due to a spread in metallicity. The values estimated by Light & Seitzer (1988) are -1.25 ± 0.3 for [Fe/H] and ~ 0.1 for σ[Fe/H].

The Yale theoretical isochrones (Green *et al.* 1987) for 5 Gyr and [Fe/H] $= -1.7$ and -0.7, which best fitted the overall shape of the RGB of Fornax (see Fig. 7), have also been used to estimate the mean and spread in metallicity. For this, the $\langle B-V \rangle$ values (after correcting for interstellar extinction) and $\sigma_I(B-V)_0$ for the various V magnitude bins of the CMD given in Table 6, as well as linear interpolation between the above mentioned isochrones, have been used. The results are given in columns 2 and 3 of Table 8. The mean values and standard deviation in [Fe/H], if σ_I is only due to a spread in metallicity, are in good agreement with the values estimated above using empirical relations. Since the same values have been estimated by Buonanno *et al.* (1985b), the present analysis confirms their result with much confidence.

Table 8. The metallicity and its spread. Standard deviations in [Fe/H] corresponding to intrinsic dispersion in $(B-V)_0$ due to metallicity spread and spread in age and metallicity are denoted by σ_1[Fe/H] and σ_2[Fe/H] respectively. $\sigma_A(B-V)_0$ is the intrinsic dispersion in $(B-V)_0$ of the RGB caused by a spread only in age.

$\sigma_R(B-V)_0$ is defined as $\sqrt{\sigma_I^2(B-V)_0 - \sigma_A^2(B-V)_0}$.

<V> (mag)	<[Fe/H]>	σ_1[Fe/H]	$\sigma_A(B-V)_0$ (mag)	$\sigma_R(B-V)_0$ (mag)	σ_2[Fe/H]
18.30			0.09	0.12	
18.54			0.09	0.12	
18.77	-1.43		0.09	0.08	
19.05	-1.55	0.28	0.08	0.13	0.24
19.28	-1.42	0.24	0.07	0.09	0.20
19.53	-1.34	0.28	0.06	0.09	0.23
19.78	-1.39	0.31	0.06	0.09	0.26
20.02	-1.45	0.34	0.05	0.10	0.31
20.29	-1.48	0.39	0.04	0.10	0.36
20.53	-1.58				
20.79	-1.58				
Mean	-1.5±0.1	0.31±0.05			0.27±0.06

3.3 Cause of the giant branch spread

Among the galactic globular clusters the best known example with a wide giant branch is ω Cen (Cannon & Stobie 1973), which appears to be possibly unique although a few other clusters may have significant spread on their GB. Intrinsic width in the giant branch has been observed not only in Fornax but also in other dwarf spheroidals, e.g. in Leo I by Fox & Pritchet (1987), and in Leo II by Demers & Harris (1983).

Recent CCD observations have indicated the presence of both old (~ 10 Gyr) and intermediate age (1–4 Gyr) stellar populations in Fornax (Buonanno *et al.* 1985b; Gratton *et al.* 1986a; Light & Seitzer 1988, and references therein). All galactic globular clusters appear to have about the same age, while the rather small number of intermediate age and old open clusters cover only a narrow range in metallicities and are too sparse to have well-defined GBs. It is therefore not yet possible to make an empirical estimate of the effects of an age spread on giant branch width, as has been done in Section 3.2 for metallicity. Using the theoretical isochrones given by Green *et al.* (1987), the predicted spread in $(B-V)$ colour of the RGB due to a range in the age of the stars can be calculated. The results of an age range from 3–17 Gyr for $Y = 0.2$ and [Fe/H] $= -1.7$ are listed in column 4 of Table 8. The results are almost the same using the isochrones for [Fe/H] $= -1.3$ instead of [Fe/H] $= -1.7$. The spread in $(B-V)$ due to variation in age σ_A is always considerably less than the total intrinsic dispersion σ_1 listed in Table 6, and consequently cannot account for the intrinsic width of the Fornax RGB. The intrinsic dispersions in $(B-V)$, σ_R, unaccounted for by such a variation in age at the different V magnitude levels, have been estimated, and are listed in column 5 of Table 8. Standard deviations in [Fe/H] equivalent to these dispersions have been estimated using the theoretical isochrones and procedure mentioned in the last section. The results are again listed in Table 8, which indicates that either a spread in metallicity alone equivalent to standard deviation of 0.31 ± 0.05 dex in [Fe/H], or both a spread in metallicity equivalent to a standard deviation of 0.27 ± 0.06 dex in [Fe/H] and a variation of 3–17 Gyr in age can account for the observed intrinsic width of the Fornax RGB.

4 THE LUMINOSITY FUNCTION

The luminosity function (LF) for the GB of the Fornax dwarf galaxy, as derived from the electronographic data in the range of $V = 18$–21.4 mag, is presented in Fig. 10 and listed in Table 9. This LF was obtained by counting the number of stars in bins 0.1 mag wide in M_V using an apparent distance modulus of 20.7 mag. It should be noted that this luminosity function will be affected both by incompleteness due to

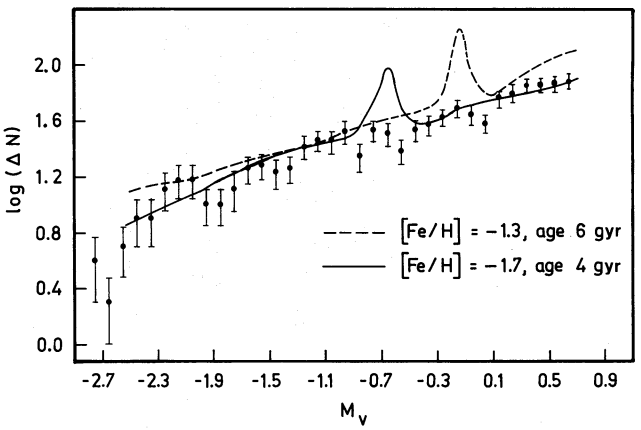

Figure 10. The luminosity function of the Fornax red giant branch. The smooth curves are theoretical luminosity functions for $Y = 0.2$ (*cf.* Green *et al.* 1987).

Table 9. The luminosity function of the Fornax red giant branch.

M_v (mag)	ΔN	M_v (mag)	ΔN
-2.8 to -2.7	4	-1.0 to -0.9	33
-2.7 to -2.6	2	-0.9 to -0.8	22
-2.6 to -2.5	5	-0.8 to -0.7	34
-2.5 to -2.4	8	-0.7 to -0.6	32
-2.4 to -2.3	8	-0.6 to -0.5	24
-2.3 to -2.2	13	-0.5 to -0.4	34
-2.2 to -2.1	15	-0.4 to -0.3	37
-2.1 to -2.0	15	-0.3 to -0.2	42
-2.0 to -1.9	10	-0.2 to -0.1	49
-1.9 to -1.8	10	-0.1 to 0.0	44
-1.8 to -1.7	13	0.0 to 0.1	38
-1.7 to -1.6	18	0.1 to 0.2	57
-1.6 to -1.5	19	0.2 to 0.3	62
-1.5 to -1.4	17	0.3 to 0.4	71
-1.4 to -1.3	18	0.4 to 0.5	71
-1.3 to -1.2	26	0.5 to 0.6	74
-1.2 to -1.1	29	0.6 to 0.7	76
-1.1 to -1.0	28	0.7 to 0.8	77

crowding and by the presence of foreground stars, although the numbers of the latter should be small (see Section 3). No corrections have been applied for these effects, so care should be taken in interpreting the overall slope of the luminosity function. However, the reasonable agreement with the theoretical luminosity functions indicate that the corrections cannot be very large.

Fig. 10 shows some deficiency of stars at $M_V = -1.9$, -0.85, -0.55 and -0.05 mag. The statistical significance of these has been estimated as follows. Inspection of Fig. 11 indicates that a line of constant slope is a reasonable approximation to the overall shape of the LF. Least-squares fitting then enables the calculation of the expected number of stars in each magnitude bin. Assuming that the star counts follow Poisson statistics, the significance levels for the above mentioned deficiencies were estimated. The deviation from the expected number of stars at $M_V = -1.9$ and -0.85 mag is less than 1σ, while at $M_V = -0.55$ and -0.05 mag, it is less than 2σ. Consequently, we conclude that these gaps are of questionable statistical significance and are probably not real features. However, it is worth pointing out here that such gaps have been observed in the GB of some galactic globular clusters although currently they are not understood theoretically (*cf.* Ratcliff 1987, and references therein).

As the theoretical isochrones which best fit to the GB of Fornax are for age = 5 Gyr and [Fe/H] between -1.7 and -1.3 (see Section 3.1.3), the present LF has been compared with theoretical ones given by Green *et al.* (1987) for these metallicities and for age close to 5 Gyr after normalizing the star counts at $M_V = -1.1$ mag. These theoretical LFs are plotted in Fig. 11. An inspection of the theoretical LFs given by Green *et al.* (1987) indicates that the slopes for the different ages are almost the same, with the theoretical LF for [Fe/H] $= -1.7$ fitting better than that for [Fe/H] $= -1.3$ to the observed LF. The observed LF is in good agreement with the theoretical one in all regions except for the peak near $M_V = 0$, which is not present in the observed data. This peak corresponds to a brief standstill in luminosity in the theoretical evolutionary track, which occurs when the hydrogen shell-burning zone encounters a composition discontinuity left behind by an earlier convective phase; it is not related to the horizontal branch. The absence of a peak in the observed LF could be because of the fact that the red giant stars of the Fornax dwarf have a large spread in metallicity and variation in age, and the position of the peak is a function of both.

5 CONCLUSIONS

BV electronographic observations of nearly 1300 stars have been used to study the detailed structure of the Fornax giant branch. Although the exceptional width of the Fornax giant branch in $(B-V)$ has been noted by earlier investigators, its extension in $(B-V)$ is quantified for the first time here. The main cause of widening of the Fornax giant branch seems to be variation in metallicity. Variations in age alone cannot account for the observed intrinsic width of the Fornax GB, although it is probable that age variations also exist and account for a small proportion of the observed scatter.

ACKNOWLEDGMENTS

We are grateful to the PDS staff at RGO for their help during the scanning of the films. Useful discussions with Dr A. J. Penny and Dr P. J. Godwin are thankfully acknowledged. RS thanks the Royal Society, London for providing the financial support through the Nuffield Foundation for this work. The observations were obtained as a subsidiary project during time awarded to two of the authors (MRSH + RDC) for another programme in collaboration with Professor K. Gyldenkerne.

REFERENCES

Aaronson, M. & Mould, J., 1980. *Astrophys. J.*, **240,** 804.
Aaronson, J. & Mould, J., 1985. *Astrophys. J.*, **290,** 191.
Alcaino, G. & Liller, W., 1981. *Astr. J.*, **86,** 1480.
Azzopardi, M. & Westerlund, B. E., 1984. *The ESO Messenger,* **36,** 12.
Bolte, M., 1987a. *Astrophys. J.*, **315,** 469.
Bolte, M., 1987b. *Astrophys. J.*, **319,** 760.
Buonanno, R., Corsi, C. E. & Fusi Pecci, F., 1981. *Mon. Not. R. astr. Soc.*, **196,** 435.
Buonanno, R., Corsi, C. E., Fusi Pecci, F., Alcaino, G. & Liller, W., 1984. *Astrophys. J.*, **277,** 220.
Buonanno, R., Corsi, C. E. & Fusi Pecci, F., 1985a. *Astr. Astrophys.*, **145,** 97.
Buonanno, R., Corsi, C. E., Fusi Pecci, F., Hardy, E. & Zinn, R., 1985b. *Astr. Astrophys.*, **152,** 65.
Buonanno. R., Buzzoni, A., Corsi, C. E., Fusi Pecci, F. & Sandage, A. R., 1986. *Mem. Soc. astr. Ital.*, **57,** 391.
Cannon, R. D. & Stobie, R. S., 1973. *Mon. Not. R. astr. Soc.*, **162,** 207.
Cudworth, K. M., 1985. *Astr. J.*, **90,** 65.
Da Costa, G. S., Mould, J. R. & Ortolani, S., 1984. *Astrophys. J.*, **282,** 125.
Danziger, I. J., 1973. *Astrophys. J.*, **181,** 641.
Demers, S. & Harris, W. E., 1983. *Astr. J.*, **88,** 329.
Demers, S. & Kunkel, W. E., 1979. *Publs astr. Soc. Pacif.*, **91,** 761.
Demers, S., Kunkel, W. E. & Hardy, E., 1979. *Astrophys. J.*, **232,** 84.
Dickens, R. J. & Rolland, A., 1972. *Mon. Not. R. astr. Soc.*, **160,** 37.
Fahlman, G. G., Richer, H. B. & VandenBerg, D. A., 1985. *Astrophys. J. Suppl.*, **58,** 225.

Fox, M. F. & Pritchet, C. J., 1987. *Astr. J.*, **93,** 1381.
Frogel, J. A., Blanco, V. M., McCarthy, M. F. & Cohen, J. G., 1982. *Astrophys. J.*, **252,** 133.
Godwin, P. J., 1986. *A study of Carina dwarf Galaxy, PhD thesis,* University of Edinburgh.
Gordon, K. C. & Kron, G. E., 1983. *Publs astr. Soc. Pacif.*, **95,** 461.
Gratton, R. G., 1987. *Astr. Astrophys.*, **179,** 181.
Gratton, R. G., Ortolani, S. & Richter, O. G., 1986a. *Mem. Soc. astr. Ital.*, **57,** 561.
Gratton, R. G., Quarta, M. L. & Ortolani, S., 1986b. *Astr. Astrophys.*, **169,** 208.
Green, E. M., Demarque, P. & King, C. R., 1987. *The Revised Yale Isochrones and Luminosity Functions,* Yale University Observatory, New Haven, Connecticut, USA.
Harris, W. E., 1982. *Astrophys. J. Suppl.*, **50,** 573.
Harris, W. E. & Racine, R., 1979. *Ann. Rev. Astr. Astrophys.*, **17,** 241.
Harris, W. E. & van den Bergh, S., 1981. *Astr. J.*, **86,** 1627.
Hawkins, M. R. S., 1981. *Mon. Not. R. astr. Soc.*, **194,** 1013.
Hesser, J. E., Harris, W. E., VandenBerg, D. A., Allwright, J. W. B., Shot, P. & Stetson, P. B., 1987. *Publs astr. Soc. Pacif.*, **99,** 739.
Jones, T. J. & Hyland, A. R., 1982. *Mon. Not. R. astr. Soc.*, **200,** 509.
Kunkel, W. E. & Demers, S., 1977. *Astrophys. J.*, **214,** 21.
Lee, S. W., 1977. *Astr. Astrophys. Suppl.*, **27,** 367.
Light, R. & Seitzer, P., 1988. *The Harlow–Shapley Symposium on Globular Cluster Systems in Galaxies, IAU Symp. No. 126,* eds Grindlay, J. E. & Philip, A. G. D., p. 583. Kluwer Academic Publishers, Dordrecht.
McClure, R., D., VandenBerg, D. A., Bell, R. A., Hesser, J. E. & Stetson, P. B., 1987. *Astr. J.*, **93,** 1144.
Penny, A. J., 1984. *Mon. Not. R. astr. Soc.*, **208,** 559.
Penny, A. J. & Dickens, R. J., 1986. *Mon. Not. R. astr. Soc.*, **220,** 845.
Pound, M. W., Janes, K. A. & Heasley, J. N., 1987. *Astr. J.*, **94,** 1185.
Ratcliff, S. J., 1987. *Astrophys. J.*, **318,** 196.
Ratnatunga, K. U. & Bahcall, J. N., 1985. *Astrophys. J. Suppl.*, **59,** 63.
Richer, H. B. & Fahlman, G. G., 1984. *Astrophys. J.*, **277,** 227.
Richer, H. B. & Fahlman, G. G., 1986. *Astrophys. J.*, **304,** 273.
Richer, H. B. & Westerlund, B. E., 1983. *Astrophys. J.*, **264,** 114.
Sagar, R., Cannon, R. D. & Hawkins, M. R. S., 1988. *Mon. Not. R. astr. Soc.*, **232,** 131.
Sandage, A. R., 1970. *Astrophys. J.*, **162,** 841.
Schommer, R. A., Olszewski, E. W. & Cudworth, K. M., 1981. *Astrophysical Parameters for Globular Clusters, IAU Colloq. No. 68,* eds Philips, A. G. D. & Hayes, D. S., p. 453. Dakis Press Inc., Schenectady, N. Y.
Shapley, H., 1938. *Nature,* **142,** 715.
Stetson, P. B., 1979. *Astr. J.*, **84,** 1149.
van den Bergh, S., 1969. *Astrophys. J. Suppl.*, **19,** 145.
Verner, G., Demers, S., Hardy, E. & Kunkel, W. E., 1981. *Astr. J.*, **86,** 357.
Wallerstein, G. Leep, E. M. & Oke, J. B., 1987. *Astr. J.*, **93,** 1137.
Westerlund, B. E., 1979. *The ESO Messenger,* **19,** 7.
Westerlund, B. E., Edvardsson, B. & Lundgren, K., 1987. *Astr. Astrophys.*, **178,** 41.
Zinn, R. & Persson, S. E., 1981. *Astrophys. J.*, **247,** 849.
Zinn, R. & West, M. J., 1984. *Astrophys. J. Suppl.*, **55,** 45.

Monthly Notices
of the
ROYAL
ASTRONOMICAL SOCIETY

VOL. 242 NO. 1, 1990

The giant branch of the Fornax dwarf spheroidal galaxy

by R. Sagar, M. R. S. Hawkins and R. D. Cannon

Published for
The Royal Astronomical Society
by
Blackwell Scientific Publications Ltd
Osney Mead
Oxford
OX2 OEL

The microfiches are 105 x 148 mm archivally permanent silver halide film produced to internationally accepted standards in the NMA 98-image format

Microfiches produced by Micromedia, Bicester, Oxon

Table 1 (on microfiche). Relative positions and electronographic BV magnitudes of stars measured in the field of the Fornax dwarf galaxy. Positions are relative to star R1-107 ($\alpha = 02^h36^m52^s.8$, $\delta = -35°00'42''$; 1950). $\Delta\alpha$ and $\Delta\delta$ in arcsec are the difference in right ascension and declination, respectively. Stars numbered by Demers & Kunkel (1979) and Verner *et al.* (1981) are prefixed by DK and *V* respectively, while those of Buonanno *et al.* (1985b) in the field area 2 are prefixed by *B* and in cluster 2 by BA.

Star	Δα (")	Δδ (")	V (mag)	(B-V) (mag)	Other Identifications	Star	Δα (")	Δδ (")	V (mag)	(B-V) (mag)	Other Identifications
					REGION 1						
1	-136	-331	21.64	-0.04		64	-115	-139	21.35	0.62	
2	-128	-307	21.04	0.63		65	-91	-146	20.85	0.73	
3	-109	-294	21.63	0.25		66	-138	-191	19.09	1.25	
4	-104	-307	17.96	0.52		67	-127	-202	21.56	0.16	
5	-103	-331	18.10	1.38		68	-123	-196	21.32	0.60	
6	-81	-328	21.55	0.54		69	-119	-185	21.51	0.35	
7	-70	-310	20.10	0.92		70	-106	-187	20.60	0.94	
8	-62	-296	21.07	0.88		71	-37	-179	20.97	0.91	
9	-62	-272	21.46	0.44		72	-51	-210	20.12	0.80	
10	-19	-277	20.80	0.57		73	-89	-239	21.46	0.44	
11	-33	-256	21.15	1.04		74	-117	-229	21.43	0.42	
12	-21	-228	20.46	0.96		75	-130	-217	20.92	1.03	
13	30	-258	21.91	0.76		76	-141	-228	21.75	0.23	
14	46	-265	20.69	1.08		77	-159	-241	19.33	1.11	
15	-14	-294	21.77	0.41		78	-168	-292	21.35	0.87	
16	-60	-325	20.70	0.61		79	-181	-267	19.23	1.59	
17	-61	-336	21.43	0.44		80	-208	-278	21.02	1.21	
18	-79	-347	21.54	0.29		81	-213	-263	21.19	0.71	
19	-81	-363	19.78	0.23		82	-210	-226	20.56	0.98	
20	-65	-362	21.55	0.23		83	-183	-210	19.72	0.90	
21	-71	-394	19.79	1.25		84	-255	-258	21.64	0.55	
22	-52	-397	21.40	0.24		85	-271	-232	19.92	0.81	
23	-30	-402	20.98	0.67		86	-246	-228	19.00	1.11	
24	6	-344	21.83	0.29		87	-227	-220	20.77	1.02	
25	7	-349	20.90	0.64		88	-216	-202	21.12	1.30	
26	27	-329	20.55	0.61		89	-190	-199	21.26	1.23	
27	32	-338	19.37	1.07		90	-212	-188	18.64	1.50	
28	42	-347	21.46	0.41		91	-226	-186	20.66	0.87	
29	56	-350	21.31	0.59		92	-210	-163	20.68	1.04	
30	94	-300	21.62	0.36		93	-267	-193	21.35	0.78	
31	23	-165	21.26	0.94		94	-266	-185	21.10	0.39	
32	35	-156	20.39	0.76		95	-282	-188	20.89	1.29	
33	70	-172	20.30	0.85		96	-305	-221	21.87	0.20	
34	77	-187	21.57	0.41		97	-315	-215	18.93	0.99	
35	104	-228	18.95	1.21		98	-317	-186	20.67	0.60	
36	123	-223	21.27	0.68		99	-304	-170	20.04	0.87	
37	206	-266	17.51	0.91		100	-295	-175	21.22	0.99	
38	252	-210	19.02	0.35		101	-289	-167	21.41	0.49	
39	250	-198	20.69	0.65		102	-28	80	21.57	0.47	
40	188	-212	19.32	1.26		103	-22	74	21.41	0.51	
41	220	-214	21.50	0.48		104	-61	48	18.12	1.44	
42	225	-207	20.41	1.00		105	-23	28	18.62	1.51	
43	261	-176	16.86	0.94		106	-17	17	19.18	0.99	
44	280	-159	16.56	1.24		107	0	1	18.27	2.54	DK7
45	236	-155	18.29	1.73		108	29	19	19.04	0.63	
46	203	-176	19.32	1.15		109	56	4	17.14	0.51	
47	158	-181	20.82	0.85		110	20	-12	19.05	1.20	
48	157	-165	19.71	0.97		111	6	-25	21.28	0.66	
49	133	-113	20.40	1.02		112	5	-45	21.09	0.97	
50	119	-117	20.70	0.64		113	21	-59	21.20	0.92	
51	133	-156	20.38	0.97		114	69	-17	18.46	1.15	
52	98	-130	18.91	1.33		115	102	-38	19.56	1.29	
53	61	-134	19.52	0.95		116	86	-66	20.94	0.73	
54	-184	-73	19.42	0.83	BA10	117	50	-58	18.93	1.28	
55	-205	-82	19.69	0.93	V13,BA1	118	18	-76	21.21	0.80	
56	-227	-106	19.50	1.38	V16	119	22	-118	20.89	0.89	
57	-222	-136	21.62	0.33		120	28	-100	21.34	0.49	
58	-178	-89	19.03	1.11	V11	121	18	-102	19.94	1.05	
59	-173	-97	20.49	0.83		122	21	-95	21.76	0.26	
60	-167	-94	21.71	0.44		123	10	-128	20.65	0.77	
61	-158	-147	19.14	1.03		124	11	-143	21.22	0.85	
62	-148	-165	20.98	0.96		125	-17	-170	20.33	0.87	
63	-123	-138	21.37	1.03		126	-12	-132	21.51	0.03	

Star	Δα (")	Δδ (")	V (mag)	(B-V) (mag)	Other Identifications	Star	Δα (")	Δδ (")	V (mag)	(B-V) (mag)	Other Identifications
127	-14	-125	21.43	0.75		134	-76	-94	21.45	0.09	
128	-31	-123	21.69	0.46		135	-81	-114	21.33	0.47	
129	-56	-130	20.19	0.68		136	-58	-2	19.55	1.05	
130	-12	-93	19.40	1.28		137	-97	-45	19.72	1.23	
131	-24	-87	17.84	1.90		138	-117	-50	19.49	1.01	
132	-60	-90	18.62	2.98	DK8	139	-114	-61	20.60	0.92	
133	-75	-85	20.38	1.42							
					REGION 2						
1	-471	-37	20.24	1.06		57	-310	66	20.51	1.05	
2	-488	-65	20.29	0.62		58	-303	78	19.94	0.87	
3	-448	-79	18.24	1.39		59	-254	86	20.74	-0.03	
4	-416	-32	20.16	1.44		60	-279	70	20.87	0.73	V70
5	-384	-37	19.22	1.03		61	-299	54	21.38	0.96	
6	-391	-59	17.53	0.94		62	-290	49	20.77	0.85	V68
7	-422	-117	21.56	0.27		63	-285	42	21.30	0.97	V66
8	-401	-132	22.05	0.14		64	-276	46	21.32	0.23	V65
9	-377	-138	21.69	0.44		65	-257	73	21.22	1.26	
10	-357	-115	21.36	1.08		66	-241	74	20.43	0.94	
11	-331	-131	21.91	-0.06		67	-233	95	21.36	0.83	
12	-328	-144	21.59	0.33		68	-226	104	21.29	1.31	
13	-356	-187	18.55	0.65		69	-202	100	20.66	0.91	
14	-302	-141	18.86	1.43		70	-191	87	21.23	0.54	
15	-311	-125	20.83	0.65		71	-199	75	19.64	1.12	
16	-323	-93	21.51	0.40		72	-206	73	20.30	0.93	
17	-313	-92	20.66	0.86		73	-226	71	20.38	1.14	
18	-314	-102	21.04	0.58		74	-222	61	20.79	0.50	V76
19	-288	-101	21.35	0.67	V24	75	-231	50	21.86	0.44	V74
20	-281	-104	19.77	1.04	V23	76	-233	39	20.40	0.89	V73
21	-260	-60	21.92	0.15		77	-267	35	21.60	0.59	V63
22	-274	-62	21.98	0.49		78	-280	22	20.71	0.85	
23	-325	-52	20.45	0.99		79	-262	17	20.98	0.95	
24	-319	-43	21.47	0.60		80	-260	4	20.89	0.97	
25	-322	-2	20.92	1.09		81	-235	8	21.10	0.59	BA102
26	-335	-15	18.16	1.52		82	-224	8	18.49	1.57	DK9,BA101
27	-358	-36	20.52	0.96		83	-224	-1	19.55	0.22	BA97
28	-368	-35	21.00	0.44		84	-229	-15	19.50	0.99	BA85
29	-378	-18	21.14	0.85		85	-218	-26	19.14	1.00	BA71
30	-419	-14	20.00	1.30		86	-214	6	21.00	1.00	BA100
31	-424	3	20.00	0.87		87	-202	-1	20.59	0.73	BA96
32	-397	3	18.53	1.23		88	-176	-22	18.56	0.62	
33	-381	14	20.04	0.92		89	-128	28	21.24	0.85	
34	-347	43	21.06	1.13		90	-140	28	20.17	0.93	
35	-396	25	21.11	0.99		91	-155	15	21.43	0.46	
36	-393	41	21.57	0.38		92	-167	7	21.34	0.71	
37	-223	181	21.70	0.48		93	-174	12	21.59	0.74	
38	-177	147	21.29	0.74		94	-177	17	20.11	0.70	
39	-202	139	20.98	0.76		95	-169	25	21.17	0.92	
40	-205	143	21.31	1.01		96	-174	31	21.33	1.08	
41	-229	155	20.62	0.96		97	-182	39	19.95	1.05	
42	-214	120	21.20	0.79		98	-179	46	18.94	1.47	
43	-221	126	18.91	1.47		99	-208	45	20.96	0.89	
44	-236	134	19.30	1.34		100	-207	35	21.62	0.58	
45	-244	142	19.61	1.20		101	-147	53	20.28	0.99	
46	-249	113	21.57	0.63		102	-138	48	21.55	0.60	
47	-259	114	20.98	0.99		103	-123	51	20.20	0.97	
48	-267	113	21.61	0.65		104	-105	49	21.69	0.53	
49	-270	147	21.15	0.80		105	-87	62	21.55	0.49	
50	-280	143	21.21	1.26		106	-81	72	20.96	1.04	
51	-292	113	21.33	0.60		107	-85	75	21.28	0.69	
52	-331	85	21.34	0.91		108	-50	88	19.64	1.28	
53	-335	80	20.40	1.15		109	-105	62	21.41	0.73	
54	-338	78	20.79	1.44		110	-120	75	19.70	0.79	
55	-323	66	21.06	0.93		111	-122	82	19.19	1.09	
56	-326	54	21.11	1.16		112	-142	84	19.26	1.21	

Star	Δα (")	Δδ (")	V (mag)	(B-V) (mag)	Other Identifications
113	-166	86	21.45	0.73	
114	-116	104	21.56	0.50	
115	-104	107	19.79	1.14	
116	-97	130	21.50	0.22	
117	-129	131	21.57	0.52	
118	-141	131	21.85	-0.02	
119	-134	115	19.14	1.33	
120	-145	107	21.07	0.84	
121	-169	117	19.90	1.16	
122	-185	121	18.71	1.55	
123	-194	125	18.71	1.36	
124	-185	127	21.63	0.83	
125	-174	137	19.98	1.01	
126	-546	192	19.94	1.10	
127	-534	175	20.62	0.80	
128	-531	169	20.01	0.97	
129	-512	173	20.49	1.42	
130	-523	160	18.39	1.58	
131	-547	151	20.29	1.13	
132	-585	153	18.73	1.38	
133	-507	150	19.59	1.67	
134	-494	143	20.53	1.02	
135	-502	128	19.10	1.37	
136	-473	120	20.15	0.97	
137	-463	139	18.43	1.94	
138	-456	130	19.32	1.15	
139	-488	92	21.04	0.62	
140	-513	81	19.57	1.14	
141	-532	69	18.51	1.43	
142	-476	74	20.29	0.60	
143	-440	85	20.19	0.98	
144	-394	79	19.68	0.98	
145	-391	70	21.09	0.76	
146	-419	59	20.30	0.95	
147	-423	54	21.31	0.48	
148	-435	67	18.76	1.50	
149	-467	61	19.52	1.37	
150	-465	50	19.14	0.92	
151	-446	18	19.62	1.24	
152	-485	21	20.79	0.98	
153	-472	-6	20.23	1.27	
154	-478	-14	19.90	1.36	
155	-487	-16	18.76	1.13	
156	-510	41	20.55	0.76	
157	-540	40	18.86	1.43	
158	-645	38	21.47	0.23	
159	-656	49	18.69	1.24	
160	-513	221	19.64	1.04	
161	-507	202	20.56	0.87	
162	-485	177	20.59	0.53	
163	-459	189	20.10	0.99	
164	-480	167	20.92	1.05	
165	-394	205	21.50	0.72	
166	-379	206	20.55	0.68	
167	-388	194	19.94	0.85	
168	-388	172	19.88	0.94	
169	-405	165	18.37	1.77	
170	-409	152	21.26	0.58	
171	-410	141	21.42	0.80	
172	-418	138	19.98	0.76	
173	-414	131	21.41	0.68	
174	-405	123	20.37	1.07	
175	-398	130	20.97	1.04	
176	-389	135	20.96	0.24	
177	-375	119	20.81	0.70	
178	-383	104	20.53	1.35	
179	-366	115	20.05	0.86	
180	-356	112	19.85	1.02	
181	-349	102	20.34	0.94	
182	-323	134	20.00	0.69	
183	-360	166	20.18	1.09	
184	-344	167	19.65	0.77	
185	-352	175	20.21	1.28	
186	-353	185	20.30	0.81	
187	-286	169	18.91	1.07	
188	-279	191	21.48	0.40	
189	-240	209	18.15	1.43	
190	-236	224	19.81	1.06	
191	-258	218	19.37	0.97	
192	-302	195	21.20	0.63	
193	-323	198	20.44	0.85	
194	-335	205	19.58	1.31	
195	-325	226	18.46	1.52	
196	-332	230	20.99	0.87	
197	-306	249	21.17	0.79	
198	-296	274	19.57	0.87	
199	-325	285	19.79	1.11	
200	-333	308	18.39	1.56	
201	-354	250	20.57	1.22	
202	-373	264	18.80	1.27	
203	-385	249	19.45	1.26	
204	-395	229	19.85	1.03	
205	-404	223	21.22	0.94	
206	-415	223	20.25	0.78	
207	-432	270	20.39	0.81	
208	-431	281	19.57	1.24	
209	-435	291	17.48	1.57	
210	-391	287	18.86	1.13	

REGION 3

Star	Δα (")	Δδ (")	V (mag)	(B-V) (mag)	Other Identifications
1	-156	252	20.87	0.74	
2	-164	241	16.26	0.93	
3	-175	222	21.22	0.76	
4	-184	211	20.11	0.79	
5	-171	214	19.94	1.18	
6	-171	208	20.85	0.64	
7	-153	219	21.39	1.05	
8	-158	229	21.25	0.72	
9	-151	235	21.30	0.51	
10	-137	244	21.09	1.01	
11	-136	234	20.37	0.88	
12	-147	229	20.33	0.85	
13	-136	223	20.55	0.92	
14	-140	206	21.34	0.80	
15	-151	186	21.33	0.85	
16	-136	188	19.37	1.20	
17	-117	227	21.12	0.83	
18	-103	208	19.69	1.01	
19	-114	186	19.64	1.06	
20	-92	177	20.40	0.74	
21	-85	178	21.58	0.77	
22	-112	166	21.08	0.87	
23	-80	180	21.64	0.83	
24	-78	175	22.32	0.17	
25	-71	175	18.25	1.87	DK13
26	-82	165	20.76	0.90	
27	-72	162	21.26	0.66	
28	-52	174	21.25	-0.08	

Star	Δα (")	Δδ (")	V (mag)	(B-V) (mag)	Other Identifications
29	-53	158	18.99	0.45	
30	-51	150	19.08	1.24	
31	-83	141	20.87	0.69	
32	-74	141	20.77	0.64	
33	-66	145	21.42	0.61	
34	-62	140	18.84	1.24	
35	-69	137	21.26	0.58	
36	-58	129	20.67	0.81	
37	-40	114	21.09	0.62	
38	-22	112	18.52	1.51	
39	-18	120	19.40	0.96	
40	-7	125	19.48	1.15	
41	-11	135	21.00	1.15	
42	-21	149	20.47	0.95	
43	-34	152	21.02	0.80	
44	-36	165	20.55	0.85	
45	26	175	19.91	1.10	
46	69	207	20.91	0.65	
47	87	213	19.56	1.21	
48	76	219	20.89	0.66	
49	78	226	21.47	0.55	
50	98	239	20.68	1.16	
51	91	242	20.48	1.04	
52	86	234	20.25	0.86	
53	69	245	19.73	1.26	
54	55	239	21.23	0.74	
55	50	234	21.22	0.76	
56	53	229	20.61	0.88	
57	63	217	20.48	0.98	
58	48	207	21.60	0.45	
59	32	206	19.68	1.14	
60	31	197	21.06	1.08	
61	18	174	21.75	0.38	
62	17	185	21.28	0.81	
63	8	191	21.43	0.54	
64	20	205	21.39	0.48	
65	8	206	20.90	1.24	
66	3	199	20.56	0.82	
67	-1	191	21.04	0.31	
68	-6	190	20.99	0.63	
69	-25	180	19.97	1.16	
70	-37	194	21.50	0.76	
71	-35	198	21.58	0.49	
72	-41	200	20.94	1.10	
73	-33	216	21.68	0.57	
74	-25	204	20.69	0.72	
75	-16	204	21.29	0.58	
76	-8	202	20.59	0.69	
77	-3	209	21.54	0.46	
78	-27	224	21.15	1.17	
79	-23	220	21.30	0.97	
80	-8	221	20.01	1.03	
81	26	232	19.53	0.95	
82	40	224	20.35	0.61	
83	35	229	21.35	0.96	
84	34	237	20.91	1.04	
85	13	232	21.64	0.54	
86	22	247	20.36	0.85	
87	19	260	19.60	1.02	
88	26	257	19.27	1.11	
89	41	257	20.86	1.72	
90	27	274	16.19	0.97	
91	41	277	21.65	0.51	
92	44	268	21.34	0.79	
93	61	271	17.44	1.71	
94	9	302	19.80	1.15	
95	3	319	19.66	1.70	
96	-1	308	20.89	1.20	
97	-2	300	20.86	0.93	
98	-4	297	21.03	1.43	
99	-27	302	21.11	0.90	
100	-25	290	20.99	0.96	
101	-18	287	19.96	0.96	
102	-31	267	19.33	1.04	
103	-23	260	22.02	0.10	
104	-24	249	20.70	1.19	
105	-29	250	21.20	1.08	
106	-50	254	20.39	0.50	
107	-58	244	21.30	0.75	
108	-41	244	18.41	1.51	
109	-52	223	21.52	0.50	
110	-58	213	21.39	0.93	
111	-75	222	21.58	0.49	
112	-75	230	19.77	0.78	
113	-67	237	21.02	0.86	
114	-60	257	21.35	0.41	
115	-92	244	21.06	0.51	
116	-94	255	21.57	0.74	
117	-125	252	19.22	1.56	
118	-128	258	21.11	0.69	
119	-136	266	21.68	0.45	
120	-124	267	21.25	0.63	
121	-127	276	21.77	0.17	
122	-125	285	21.14	0.79	
123	-113	296	21.65	0.34	
124	-109	289	20.37	1.05	
125	-102	284	20.51	0.84	
126	-102	278	20.27	0.95	
127	-76	281	18.63	1.58	
128	-56	310	20.03	0.81	
129	-88	288	20.97	1.00	
130	-99	308	19.75	1.12	
131	-75	327	20.14	1.12	
132	-60	343	18.57	1.53	
133	-40	348	18.53	1.52	
134	-44	328	20.79	0.82	
135	-35	321	20.93	1.08	
136	123	471	19.61	1.16	
137	110	453	21.90	0.45	
138	103	448	19.92	1.04	
139	103	441	20.80	1.21	
140	86	473	20.69	0.83	
141	69	452	19.87	1.16	
142	59	449	21.38	0.24	
143	75	444	21.06	0.85	
144	66	438	20.25	1.09	
145	44	435	19.43	1.10	
146	38	428	20.67	0.73	
147	34	426	21.03	1.16	
148	38	410	20.43	0.99	
149	12	394	19.88	1.09	
150	9	390	21.32	1.13	
151	1	390	21.07	0.87	
152	-10	377	21.35	0.91	
153	-18	360	21.17	1.16	
154	-12	360	20.97	0.64	
155	-5	350	21.03	1.07	
156	5	359	20.97	0.75	
157	23	366	20.54	0.94	
158	46	376	21.22	0.67	
159	52	380	21.42	0.57	
160	57	387	21.59	0.34	

Star	Δα (")	Δδ (")	V (mag)	(B-V) (mag)	Other Identifications
161	55	398	19.93	1.24	
162	71	413	19.93	1.10	
163	81	425	21.33	0.63	
164	108	432	20.27	1.16	
165	92	387	19.84	1.13	
166	82	391	21.10	0.88	
167	82	382	21.41	0.20	
168	68	384	18.00	1.17	
169	73	378	19.77	1.18	
170	77	362	18.50	1.71	
171	67	363	21.34	0.91	
172	46	342	21.49	0.20	
173	24	353	21.49	0.25	
174	19	349	21.40	0.48	
175	40	331	18.30	1.75	
176	47	334	21.48	0.72	
177	61	334	20.30	1.15	
178	40	314	18.72	1.50	
179	48	305	20.97	1.01	
180	69	320	20.44	0.77	
181	79	326	21.89	0.27	
182	112	352	18.43	1.74	
183	111	333	20.76	1.26	
184	103	325	18.76	1.46	
185	97	318	20.66	0.89	
186	89	320	21.28	0.89	
187	85	305	19.80	1.12	
188	79	295	21.07	0.99	
189	93	295	19.05	1.53	
190	104	288	19.07	0.70	
191	106	310	21.15	0.65	
192	124	323	19.88	1.08	
193	133	328	20.50	0.86	
194	121	314	20.75	0.61	
195	115	303	19.42	1.33	
196	113	295	19.19	1.13	
197	126	300	21.34	0.85	
198	131	307	20.96	0.80	
199	142	315	20.92	1.21	
200	153	301	21.13	0.99	
201	161	305	21.30	0.77	
202	182	292	20.08	1.07	
203	152	284	20.03	1.09	
204	132	285	21.42	0.49	
205	133	268	21.31	0.99	
206	129	254	20.02	1.05	
207	122	245	19.67	1.08	
208	121	254	18.61	1.18	
209	116	258	20.36	0.95	
210	114	269	20.48	0.84	
211	114	276	21.24	1.27	
212	101	267	20.43	0.87	
213	186	313	20.74	1.21	
214	195	325	21.13	0.85	
215	173	318	21.24	0.54	
216	150	318	20.67	0.97	
217	170	334	19.26	1.25	
218	146	331	21.22	1.06	
219	154	338	21.24	0.96	
220	157	349	19.91	1.01	
221	172	366	20.40	1.26	
222	171	362	20.60	1.02	
223	178	361	20.68	1.15	
224	177	355	21.27	0.95	
225	187	348	20.62	1.27	
226	234	340	18.59	1.67	
227	199	353	21.04	1.05	
228	211	361	21.02	1.13	
229	219	371	21.46	0.93	
230	227	367	20.70	0.59	
231	244	369	21.72	-0.07	
232	260	386	18.50	1.69	
233	221	394	19.19	1.31	
234	198	386	20.84	0.96	
235	197	390	21.35	0.82	
236	196	394	21.69	0.68	
237	193	369	20.90	0.90	
238	182	378	18.99	1.14	
239	176	388	20.82	0.76	
240	177	393	21.50	0.82	
241	167	387	21.11	1.05	
242	165	393	21.25	0.46	
243	164	380	20.09	0.63	
244	155	378	20.44	0.52	
245	153	386	18.01	0.40	
246	143	373	20.27	1.08	
247	124	378	19.78	1.06	
248	116	379	18.57	1.32	
249	120	395	19.96	1.22	
250	130	398	20.70	0.86	
251	134	374	22.02	0.23	
252	138	388	20.64	0.79	
253	141	404	21.49	0.71	
254	149	394	20.50	1.04	
255	154	409	19.87	1.11	
256	161	418	19.08	1.15	
257	190	438	21.73	0.36	
258	149	425	20.49	0.91	
259	147	417	20.37	1.06	
260	131	413	20.38	0.74	
261	118	420	21.45	0.54	
262	127	425	20.15	0.99	
263	138	420	20.60	0.78	
264	-360	347	21.01	1.02	
265	-343	346	21.08	0.73	
266	-335	361	21.56	0.60	
267	-332	371	18.58	1.50	
268	-329	362	21.13	1.05	
269	-321	359	20.88	0.69	
270	-309	356	20.85	1.20	
271	-296	365	21.39	-0.09	
272	-288	348	21.07	0.90	
273	-299	343	21.50	0.89	
274	-316	339	20.18	1.04	
275	-298	328	20.89	0.84	
276	-294	320	21.46	0.77	
277	-280	300	20.43	0.87	
278	-246	314	21.29	0.56	
279	-239	293	21.82	0.47	
280	-243	288	21.18	0.39	
281	-254	288	20.63	0.78	
282	-265	277	21.62	0.90	
283	-252	279	21.41	0.35	
284	-211	295	19.05	1.07	
285	-201	293	21.56	0.42	
286	-194	285	20.51	1.06	
287	-196	268	21.56	0.57	
288	-223	252	21.07	0.77	
289	-212	253	20.29	0.81	
290	-203	253	21.32	0.89	
291	-193	258	21.32	0.62	
292	-188	247	20.75	0.74	

Star	Δα (")	Δδ (")	V (mag)	(B-V) (mag)	Other Identifications
293	-172	269	19.93	1.07	
294	-162	277	19.85	1.00	
295	-163	286	21.58	0.68	
296	-154	289	21.94	0.37	
297	-145	290	21.24	0.78	
298	-140	290	20.95	0.82	
299	-156	295	19.51	1.11	
300	-169	315	21.07	0.65	
301	-163	311	21.35	0.93	
302	-159	306	21.42	0.53	
303	-148	312	21.18	0.62	
304	-138	312	21.78	0.33	
305	-118	309	19.81	1.42	
306	-115	320	18.50	1.23	
307	-130	333	20.84	1.15	
308	-133	338	21.04	1.27	
309	-152	334	17.67	1.03	
310	-171	342	21.00	0.61	
311	-188	316	18.58	1.54	
312	-195	323	21.46	0.66	
313	-213	329	21.08	0.82	
314	-219	345	21.76	0.48	
315	-214	345	21.39	0.81	
316	-196	354	21.16	0.90	
317	-202	361	21.11	0.86	
318	-255	343	20.81	1.05	
319	-263	339	18.87	1.46	
320	-264	367	21.20	0.76	
321	-255	369	20.83	0.94	
322	-294	381	20.99	0.76	
323	-288	397	20.46	1.04	
324	-280	408	21.55	0.48	
325	-295	420	21.34	0.77	
326	-286	423	21.14	0.92	
327	-279	433	21.50	0.64	
328	-273	424	21.12	0.86	
329	-264	438	21.56	0.41	
330	-254	431	21.57	0.58	
331	-254	409	21.49	0.17	
332	-241	410	21.31	0.73	
333	-226	405	20.83	0.83	
334	-235	390	21.48	1.16	
335	-239	383	21.31	1.07	
336	-218	368	20.91	1.11	
337	-217	391	21.03	0.72	
338	-208	398	20.74	0.87	
339	-204	387	21.18	0.99	
340	-196	383	21.53	0.93	
341	-183	371	20.55	1.13	
342	-173	365	18.54	1.51	
343	-160	369	19.87	1.15	
344	-154	378	20.94	0.89	
345	-149	383	20.52	1.35	
346	-171	383	19.95	1.00	
347	-162	395	18.56	1.48	
348	-152	396	19.33	1.52	
349	-166	400	20.64	1.10	
350	-176	394	20.22	1.05	
351	-188	402	19.48	1.30	
352	-177	403	22.01	0.28	
353	-187	421	20.08	1.00	
354	-204	408	21.31	1.17	
355	-213	420	21.39	1.17	
356	-222	417	21.12	1.07	
357	-196	430	20.05	1.14	
358	-244	437	21.44	0.82	
359	-237	450	21.12	0.94	
360	-254	450	21.12	0.58	
361	-228	457	20.70	0.95	
362	-205	459	21.37	0.60	
363	-209	454	21.64	0.26	
364	-219	446	22.23	0.18	
365	-202	450	20.53	0.93	
366	-183	439	21.28	0.41	
367	-161	436	21.61	0.60	
368	-151	436	21.26	0.89	
369	-163	419	21.34	0.47	
370	-158	414	20.90	1.24	
371	-140	417	20.34	0.83	
372	-117	400	21.47	0.41	
373	-108	402	21.31	0.75	
374	-120	387	19.62	1.02	
375	-93	390	20.50	0.98	
376	-88	376	20.71	0.98	
377	-95	365	21.37	0.87	
378	-107	353	21.00	0.81	
379	-110	346	21.30	0.66	
380	-103	348	21.22	1.11	
381	-99	334	21.50	1.23	
382	-77	359	21.18	0.71	
383	-191	512	20.27	1.07	
384	-189	508	19.75	1.09	
385	-190	501	21.21	0.81	
386	-197	486	20.17	0.84	
387	-192	490	20.51	0.67	
388	-183	493	19.23	1.19	
389	-179	487	21.73	0.52	
390	-184	483	20.94	1.00	
391	-193	477	19.19	1.01	
392	-173	483	20.93	0.80	
393	-150	478	19.97	0.67	
394	-150	486	20.71	0.85	
395	-138	489	18.35	1.85	
396	-122	485	19.43	1.21	
397	-129	468	16.48	1.69	
398	-124	458	20.24	1.00	
399	-114	450	21.21	0.69	
400	-148	445	19.45	1.23	
401	-116	426	20.73	0.87	
402	-104	421	20.70	0.68	
403	-99	419	20.32	1.13	
404	-86	428	20.98	1.12	
405	-87	425	21.90	0.47	
406	-74	413	20.48	0.70	
407	-66	415	18.99	1.22	
408	-67	408	19.81	1.17	
409	-60	354	19.92	1.06	
410	-45	399	20.80	0.65	
411	-39	379	21.06	0.96	
412	-8	408	18.70	1.49	
413	-19	409	21.53	0.59	
414	-44	413	19.13	1.19	
415	-36	421	21.15	1.00	
416	-22	425	20.04	0.30	
417	-9	425	19.12	1.18	
418	-3	428	19.36	1.30	
419	2	421	20.57	0.88	
420	11	430	20.22	1.08	
421	26	443	20.49	1.04	
422	11	453	19.61	1.10	
423	8	459	19.16	1.11	
424	3	452	19.86	1.06	

Star	Δα (")	Δδ (")	V (mag)	(B-V) (mag)	Other Identifications	Star	Δα (")	Δδ (")	V (mag)	(B-V) (mag)	Other Identifications
425	-11	447	20.44	0.76		475	-94	548	21.71	0.79	
426	-19	439	19.08	1.29		476	-86	548	20.97	0.93	
427	-16	432	20.29	0.91		477	-103	527	21.15	0.89	
428	-33	444	21.00	1.09		478	-96	528	20.87	0.40	
429	-39	449	20.44	1.09		479	-87	533	21.05	0.95	
430	-44	453	21.15	0.45		480	-82	537	20.89	1.10	
431	-47	459	21.50	0.84		481	-75	531	18.69	1.24	
432	-53	455	21.50	0.91		482	-83	528	20.55	1.26	
433	-57	453	21.62	0.38		483	-72	540	21.60	0.97	
434	-53	448	21.57	0.33		484	-70	547	20.65	0.79	
435	-64	449	19.34	1.20		485	-44	544	21.50	0.66	
436	-70	447	20.01	1.44		486	-52	532	20.58	0.85	
437	-72	444	21.44	0.69		487	-38	520	20.74	0.84	
438	-80	450	20.82	0.75		488	-28	521	21.32	0.64	
439	-73	434	21.29	0.77		489	-33	510	21.20	0.85	
440	-75	461	20.54	0.74		490	-24	503	19.55	1.35	
441	-56	478	20.52	1.07		491	-13	498	20.89	0.82	
442	-66	470	20.26	1.15		492	-19	498	21.25	0.89	
443	-69	486	20.92	1.13		493	-21	463	21.49	0.49	
444	-89	489	19.45	1.28		494	14	489	20.17	0.97	
445	-103	475	18.70	1.37		495	11	493	19.30	1.52	
446	-103	468	19.21	1.51		496	48	485	21.37	0.89	
447	-79	498	19.56	1.07		497	53	482	20.87	0.78	
448	-90	509	18.68	1.47		498	55	476	20.90	0.87	
449	-116	513	20.25	1.20		499	57	471	21.22	0.78	
450	-110	513	21.03	0.42		500	49	466	19.72	0.95	
451	-107	507	18.57	1.52		501	70	495	18.30	1.92	
452	-127	509	20.51	1.10		502	52	498	19.92	1.16	
453	-155	504	18.27	1.67		503	52	504	19.13	1.42	
454	-148	500	21.54	0.38		504	28	511	20.28	1.71	
455	-163	519	18.50	1.36		505	21	525	19.69	1.27	
456	-173	530	21.47	0.58		506	-13	539	16.90	1.29	
457	-155	532	21.22	1.05		507	-19	535	20.94	1.13	
458	-149	523	20.83	0.75		508	-19	556	19.43	1.35	
459	-143	520	19.20	1.39		509	-18	576	19.13	1.11	
460	-128	523	20.39	0.52		510	-30	572	20.02	1.00	
461	-120	529	18.50	1.74		511	-35	569	21.15	0.96	
462	-114	534	21.40	0.45		512	-48	571	20.02	1.22	
463	-106	538	20.02	1.02		513	-60	564	19.56	0.61	
464	-113	541	21.02	0.75		514	-73	558	20.00	1.06	
465	-109	548	20.31	0.92		515	-75	565	20.16	1.02	
466	-107	558	21.11	1.00		516	-40	604	21.65	0.15	
467	-120	551	18.25	1.80		517	-49	603	19.43	1.34	
468	-142	542	19.48	1.12		518	-73	586	20.76	0.94	
469	-128	563	21.26	0.96		519	-65	591	21.45	0.96	
470	-106	582	19.74	1.15		520	-68	596	21.29	0.64	
471	-81	580	19.45	1.27		521	-65	606	19.56	1.25	
472	-88	573	21.17	0.80		522	-53	610	20.21	1.17	
473	-87	567	21.49	0.70		523	-71	617	21.35	0.47	
474	-102	548	21.07	0.83							

REGION 4

1	162	-34	20.06	1.05		14	271	-69	19.28	1.31	
2	173	-39	21.11	1.10		15	252	-85	21.31	0.80	
3	203	-27	20.67	1.17		16	254	-105	21.59	0.28	
4	194	-32	18.70	1.49		17	265	-98	19.49	1.40	
5	196	-51	20.31	0.97		18	271	-102	20.35	1.00	
6	212	-58	20.96	0.81		19	263	-113	19.43	1.24	
7	220	-50	19.27	1.24		20	270	-119	21.14	0.87	
8	236	-54	21.25	0.79		21	293	-93	20.82	0.77	
9	245	-56	21.08	0.64		22	303	-87	20.42	1.00	
10	249	-57	20.55	0.98		23	294	-98	20.52	0.75	
11	250	-48	21.67	0.83		24	316	-84	21.17	0.97	
12	258	-50	21.51	0.26		25	321	-99	20.81	0.99	
13	268	-48	21.55	-0.10		26	312	-107	20.79	1.73	

Star	Δα (")	Δδ (")	V (mag)	(B-V) (mag)	Other Identifications
27	327	-144	21.49	0.50	
28	347	-117	20.79	1.12	
29	351	-119	21.59	0.08	
30	365	-115	19.57	0.98	
31	368	-111	19.46	1.29	
32	328	-85	20.56	0.90	
33	394	-63	20.40	1.29	
34	404	-42	21.46	0.02	
35	403	-34	20.28	1.16	
36	418	-23	18.38	1.58	
37	418	-7	19.41	1.05	
38	436	-5	21.30	0.76	
39	392	-26	19.82	1.09	
40	334	-65	20.76	0.72	
41	322	-67	20.54	0.82	
42	309	-70	21.20	0.76	
43	285	-64	21.26	0.70	
44	296	-57	19.12	1.27	
45	314	-56	20.87	1.17	
46	331	-56	20.23	1.00	
47	344	-44	21.23	0.71	
48	331	-41	21.04	0.93	
49	355	-36	20.44	1.10	
50	371	-24	21.18	0.83	
51	378	-17	19.87	1.26	
52	379	-9	19.68	0.88	
53	405	11	18.68	1.45	
54	398	24	19.53	1.10	
55	377	22	20.80	1.12	
56	355	-2	20.01	1.14	
57	336	-26	20.39	1.14	
58	331	-28	20.60	0.82	
59	327	-22	20.49	0.74	
60	318	-30	19.00	1.25	
61	283	-42	21.04	0.78	
62	283	-29	17.60	1.94	DK6
63	324	-13	21.87	0.30	
64	313	0	20.13	1.34	
65	305	-3	21.18	0.79	
66	293	-7	21.56	0.86	
67	302	12	20.94	0.90	
68	324	17	19.52	1.14	
69	327	26	20.58	1.11	
70	347	26	21.05	0.96	
71	364	40	19.77	0.94	
72	368	46	21.34	1.21	
73	323	35	21.50	1.06	
74	316	46	18.89	1.17	
75	301	40	20.66	0.64	
76	297	26	20.99	0.66	
77	284	18	20.00	1.00	
78	284	32	20.40	1.58	
79	282	35	21.19	0.36	
80	271	37	20.78	1.17	
81	231	-28	21.27	0.65	
82	241	-2	19.80	1.20	
83	230	-3	19.28	1.33	
84	219	0	21.30	0.58	
85	194	-11	21.45	0.94	
86	226	14	21.41	0.68	
87	227	23	21.20	1.05	
88	238	27	20.98	0.82	
89	256	47	21.55	0.51	
90	290	64	21.31	1.07	
91	306	64	20.82	0.81	
92	307	74	20.32	0.64	
93	316	82	21.44	0.25	
94	341	124	20.40	1.16	
95	326	117	21.80	0.29	
96	329	113	20.94	0.88	
97	338	115	20.73	0.98	
98	320	98	20.88	0.68	
99	347	102	20.55	1.08	
100	356	106	20.79	0.86	
101	359	115	18.86	0.94	
102	364	104	19.76	0.98	
103	386	108	21.13	0.63	
104	391	100	19.74	1.15	
105	372	88	19.70	1.28	
106	352	82	20.90	1.04	
107	416	62	18.87	1.32	
108	391	51	19.69	0.79	
109	432	45	21.27	0.92	
110	445	47	20.84	0.81	
111	455	40	21.43	0.62	
112	433	31	21.61	0.52	
113	454	25	21.82	0.10	
114	450	5	20.35	0.72	
115	489	18	19.69	0.88	
116	496	28	21.04	0.98	
117	468	43	21.62	0.44	
118	512	31	21.93	0.02	
119	532	63	20.20	1.11	
120	517	66	18.47	1.04	
121	577	93	21.77	0.52	
122	559	93	20.83	1.06	
123	535	89	19.58	0.98	
124	547	100	20.53	0.69	
125	555	124	21.66	0.46	
126	529	147	21.31	0.72	
127	527	114	21.33	0.82	
128	510	123	21.19	0.68	
129	500	112	21.39	0.75	
130	502	104	20.26	0.74	
131	485	85	21.04	0.69	
132	467	82	20.43	1.30	
133	452	77	21.67	0.41	
134	471	95	20.74	0.87	
135	483	106	17.92	1.55	
136	476	135	21.17	0.97	
137	463	141	21.04	0.99	
138	434	139	21.60	0.29	
139	431	146	21.22	0.75	
140	433	116	20.55	0.97	
141	424	111	21.48	0.51	
142	404	115	21.16	0.98	
143	391	127	20.91	0.74	
144	408	132	19.41	1.31	
145	375	119	19.58	1.10	
146	369	120	20.20	1.09	
147	361	133	20.07	0.80	
148	383	128	21.59	0.51	
149	388	138	21.06	0.29	
150	407	143	21.93	-0.11	
151	400	146	21.14	0.29	
152	411	153	21.30	0.82	
153	412	190	18.89	1.36	
154	419	184	20.99	0.89	
155	425	196	17.90	1.85	DK24
156	441	194	20.82	0.80	
157	435	173	19.07	1.36	
158	460	168	19.73	1.16	

Star	Δα (")	Δδ (")	V (mag)	(B-V) (mag)	Other Identifications
159	448	151	20.14	0.97	
160	473	168	19.76	1.16	
161	478	154	21.13	0.81	
162	471	148	21.78	0.39	
163	494	184	19.46	1.13	
164	135	223	20.82	0.74	
165	127	224	21.11	1.02	
166	130	206	19.53	1.11	
167	130	200	21.22	0.83	
168	139	206	20.99	0.97	
169	120	194	20.45	-0.13	
170	120	186	20.48	0.89	
171	129	181	20.98	1.28	
172	129	169	21.11	1.06	
173	124	174	20.95	0.77	
174	90	179	21.11	0.89	
175	82	163	21.32	0.80	
176	87	154	21.55	0.70	
177	88	141	20.86	0.83	
178	70	126	20.65	0.52	
179	64	142	21.40	0.49	
180	60	159	21.02	0.74	
181	54	142	20.47	0.98	
182	44	144	18.12	1.91	DK11
183	39	134	18.34	1.77	DK12
184	46	129	19.72	1.27	
185	27	123	19.79	0.98	
186	8	118	20.53	0.78	
187	1	102	20.65	0.62	
188	4	97	21.74	0.98	
189	-6	77	21.85	0.33	
190	16	89	21.59	0.51	
191	31	95	21.62	0.55	
192	27	105	21.79	0.27	
193	48	101	19.75	0.94	
194	62	96	21.16	0.92	
195	36	90	21.23	0.81	
196	37	78	19.81	1.19	
197	12	74	20.61	0.79	
198	19	69	21.18	1.03	
199	48	85	21.05	1.19	
200	50	75	21.67	0.43	
201	55	64	21.44	0.51	
202	40	49	21.72	0.08	
203	81	81	20.22	0.78	
204	83	109	21.55	0.28	
205	87	114	20.99	0.63	
206	109	141	20.02	1.00	
207	113	152	21.20	0.93	
208	128	130	20.47	0.93	
209	126	118	19.62	1.03	
210	128	105	19.62	1.05	
211	116	103	21.59	0.85	
212	114	100	21.31	0.62	
213	110	101	21.07	0.69	
214	149	127	21.45	1.22	
215	144	129	21.23	0.82	
216	140	144	21.04	0.71	
217	127	146	19.39	1.39	
218	125	152	17.97	0.55	
219	134	153	21.50	0.97	
220	177	140	18.78	1.50	B9
221	167	150	21.43	0.71	
222	172	157	20.89	0.88	
223	171	163	20.72	1.40	
224	183	165	20.64	0.94	B28
225	155	168	19.42	1.15	B32
226	145	179	20.60	0.86	
227	151	185	21.19	0.55	
228	163	182	20.46	0.98	B39
229	166	188	19.65	1.32	B52
230	173	193	19.51	1.05	B57
231	188	183	19.06	1.12	B43
232	198	169	20.65	0.84	B33
233	224	139	19.05	1.42	B8
234	211	143	19.18	1.27	
235	208	140	20.96	0.81	
236	214	124	21.11	0.49	
237	214	112	20.66	0.77	
238	192	106	20.49	0.68	
239	191	120	16.79	1.15	
240	181	118	19.23	1.31	
241	178	126	21.18	0.81	
242	198	134	20.77	0.73	B5
243	164	118	18.62	1.50	
244	169	114	21.03	0.74	
245	167	109	21.31	0.91	
246	150	96	19.25	1.38	
247	163	76	21.25	0.88	
248	133	74	20.64	0.61	
249	131	67	21.47	0.58	
250	109	83	21.09	1.28	
251	111	56	20.75	0.65	
252	97	54	19.79	1.24	
253	91	47	21.04	0.92	
254	84	49	19.79	1.05	
255	67	27	20.79	1.09	
256	83	28	21.49	0.59	
257	104	21	21.14	0.70	
258	115	22	18.75	1.50	
259	115	11	21.09	1.38	
260	107	5	20.69	0.84	
261	118	-3	20.57	0.87	
262	121	-4	20.49	1.04	
263	133	-19	21.22	0.97	
264	144	-18	20.33	1.05	
265	149	-15	20.00	1.11	
266	155	-2	21.35	0.83	
267	161	0	21.43	1.35	
268	170	8	18.33	1.53	
269	175	-7	21.45	0.74	
270	147	-30	20.84	0.60	
271	192	29	20.85	0.71	
272	195	37	20.94	0.83	
273	136	20	21.57	0.90	
274	147	42	20.98	1.06	
275	150	54	21.02	1.00	
276	169	66	21.58	0.65	
277	165	58	21.40	0.91	
278	161	53	20.70	0.96	
279	175	56	19.24	0.99	
280	183	48	20.49	0.93	
281	191	55	20.05	1.14	
282	184	66	21.01	0.79	
283	192	80	20.80	1.12	
284	195	86	21.57	0.49	
285	208	81	20.74	0.86	
286	223	99	20.48	0.83	
287	230	97	19.65	1.07	
288	232	92	20.72	0.87	
289	228	75	21.45	0.52	
290	261	79	19.73	0.69	

Star	Δα (")	Δδ (")	V (mag)	(B-V) (mag)	Other Identifications
291	284	100	20.04	0.95	
292	285	107	21.67	0.46	
293	263	97	19.18	1.12	
294	253	101	19.60	1.16	
295	244	108	21.24	0.77	
296	256	120	21.39	0.78	
297	263	128	21.69	0.21	
298	269	118	20.12	0.89	
299	319	127	21.23	0.27	
300	315	132	21.60	0.47	
301	315	140	18.38	1.51	
302	308	144	21.42	1.02	
303	293	123	21.28	0.96	
304	282	134	19.04	1.17	B6
305	285	144	21.00	0.33	
306	295	153	20.00	1.03	B18
307	308	174	21.48	0.38	
308	316	170	21.39	0.92	
309	322	177	20.92	0.66	
310	322	171	19.66	1.03	
311	326	166	21.37	0.79	
312	347	152	19.87	0.90	
313	376	178	19.15	1.22	
314	353	179	19.59	0.97	
315	345	190	19.46	1.06	
316	339	189	20.09	0.94	
317	328	193	20.20	0.92	
318	345	205	20.88	0.54	
319	356	209	18.49	1.19	
320	362	196	19.74	1.01	
321	374	224	20.06	0.99	
322	408	219	21.06	1.04	
323	423	220	19.76	1.05	
324	432	254	19.77	1.14	
325	374	240	21.15	0.72	
326	396	276	19.31	1.32	
327	383	281	16.96	1.43	
328	352	236	20.64	0.74	
329	349	224	19.81	0.89	
330	321	207	21.06	0.80	
331	308	210	21.05	0.88	
332	301	213	21.27	0.92	
333	308	226	20.59	1.27	
334	323	246	20.41	0.77	
335	321	256	20.26	0.79	
336	318	252	21.10	1.09	
337	308	251	21.36	0.85	B123
338	308	237	21.30	0.55	
339	296	235	20.28	0.91	B100
340	288	238	19.47	1.12	B106
341	267	240	19.38	1.28	B109
342	277	238	20.61	0.85	B108
343	289	222	20.34	0.96	
344	287	212	20.10	0.97	B78
345	283	198	21.03	0.98	
346	274	194	21.04	0.88	
347	272	201	20.50	1.13	
348	270	202	21.47	0.21	
349	277	207	20.85	1.07	B68
350	265	208	20.52	0.89	B70
351	250	199	20.85	1.16	B62
352	255	196	21.48	0.71	B59
353	250	188	20.66	0.95	
354	259	187	19.92	0.94	B47
355	261	183	20.96	0.86	B42
356	261	167	18.81	1.39	B31
357	242	173	21.23	1.09	
358	236	171	21.04	0.79	
359	224	171	20.05	1.04	B34
360	216	188	20.39	0.90	B51
361	229	193	18.17	1.47	B55
362	213	203	18.69	1.44	B66
363	202	213	20.84	0.52	B76
364	196	217	19.91	1.34	B84
365	186	201	18.51	1.50	B63
366	183	213	20.51	1.09	B77
367	175	214	21.70	0.93	B79
368	168	210	20.03	0.97	B71
369	142	240	19.53	1.91	
370	156	239	20.95	0.79	B104
371	170	240	21.02	0.79	B108
372	174	261	21.38	0.70	
373	185	255	21.34	1.08	B125
374	193	247	20.87	0.73	B118
375	199	232	19.69	1.40	B95
376	230	234	21.35	0.90	B98
377	244	215	19.26	1.35	B82
378	252	218	18.98	1.43	B86
379	251	226	21.34	0.56	B90
380	259	234	20.87	1.00	B99
381	258	244	21.38	0.64	B114
382	243	246	21.42	0.33	B117
383	235	262	20.09	1.21	
384	227	274	19.88	1.03	
385	220	294	20.16	0.94	
386	200	276	19.97	1.09	
387	199	288	20.91	0.92	
388	216	309	18.65	1.48	
389	239	294	21.15	1.79	
390	248	298	21.13	0.73	
391	268	298	21.55	0.66	
392	262	273	21.01	0.80	
393	272	278	19.60	1.26	
394	275	274	19.46	1.09	
395	270	261	19.92	1.08	
396	289	273	20.12	1.17	
397	299	267	21.68	-0.02	
398	304	260	19.32	1.22	
399	321	269	20.44	0.96	
400	319	277	22.20	0.11	
401	324	280	20.84	0.92	
402	340	265	21.47	0.38	
403	336	275	21.61	0.35	
404	308	286	20.57	0.90	
405	275	293	19.02	0.99	
406	277	302	20.75	0.71	
407	290	313	21.02	1.07	
408	318	328	17.23	0.71	
409	274	317	20.90	0.59	
410	267	309	19.98	1.07	
411	259	319	21.05	0.57	
412	267	320	21.25	0.95	
413	272	326	21.46	0.72	
414	260	333	19.10	0.96	
415	289	354	19.35	1.20	